เซลล์แสงอาทิตย์ชนิดสีย้อมไวแสงที่มี TiO_2 อิเล็กโตรดซึ่งปรับปรุงด้วย ZrO_2, CeO_2, หรือ ZnO

นางสาวอัญชนา กิตติธเนศวร

วิทยานิพนธ์นี้เป็นส่วนหนึ่งของการศึกษาตามหลักสูตรปริญญาวิศวกรรมศาสตรมหาบัณฑิต
สาขาวิชาวิศวกรรมเคมี ภาควิชาวิศวกรรมเคมี
คณะวิศวกรรมศาสตร์ จุฬาลงกรณ์มหาวิทยาลัย
ปีการศึกษา 2554

DYE-SENSITIZED SOLAR CELLS WITH TiO_2 ELECTRODE MODIFIED BY ZrO_2, CeO_2, OR ZnO

Miss Anchana Kittitanesuan

A Thesis Submitted in Partial Fulfillment of the Requirements
for the Degree of Master of Engineering Program in Chemical Engineering
Department of Chemical Engineering
Faculty of Engineering
Chulalongkorn University
Academic Year 2011

Thesis Title	DYE-SENSITIZED SOLAR CELLS WITH TiO_2 ELECTRODE MODIFIED BY ZrO_2,CeO_2, OR ZnO
By	Miss Anchana Kittitanesuan
Field of Study	Chemical Engineering
Thesis Advisor	Akawat Sirisuk, Ph.D.

Accepted by the Faculty of Engineering, Chulalongkorn University in Partial Fulfillment of the Requirements for the Master's Degree

…….....Dean of the Faculty of Engineering
(Associate Professor Boonsom Lerdhirunwong, Dr.Ing.)

THESIS COMMITTEE

……Chairman
(Professor Piyasan Praserthdam, Dr.Ing.)

…….....Thesis Advisor
(Akawat Sirisuk, Ph.D.)

……Examiner
(Professor Suthichai Assabumrungrat, Ph.D.)

……External Examiner
(Nattaya Comsup, D.Eng.)

อัญชนา กิตติธเนศวร : เซลล์แสงอาทิตย์ชนิดสีย้อมไวแสงที่มี TiO_2 อิเล็กโตรดซึ่งปรับปรุงด้วย ZrO_2, CeO_2, หรือ ZnO. (DYE-SENSITIZED SOLAR CELLS WITH TiO_2 ELECTRODE MODIFIED BY ZrO_2, CeO_2, OR ZnO) อ.ที่ปรึกษาวิทยานิพนธ์หลัก: อ.ดร.อัครวัต ศิริสุข, 62 หน้า.

งานวิจัยนี้ได้พิจารณาการเติมเซอร์โคเนียมออกไซด์, ซีเรียมออกไซด์, หรือซิงค์ออกไซด์เป็นอิเล็กโตรดสำหรับเซลล์แสงอาทิตย์ชนิดสีย้อมไวแสง และอิทธิพลของอิเล็กโตรดแบบสองชั้นที่มีผลต่อประสิทธิภาพของเซลล์แสงอาทิตย์ชนิดสีย้อมไวแสง ซึ่งสังเคราะห์ขึ้นด้วยวิธีโซล-เจล และพ่นเคลือบลงบนกระจก FTO ด้วยเครื่องพ่นอัลตร้าโซนิคจำนวน 500 รอบ จากนั้นนำไปเผาที่อุณหภูมิ 400 องศาเซลเซียส เป็นเวลาสองชั่วโมง โดยปริมาณการเติมของเซอร์โคเนียมออกไซด์อยู่ในช่วงร้อยละ 0 ถึง 10 โดยน้ำหนัก ส่วนซีเรียมออกไซด์ และซิงค์ออกไซด์อยู่ในช่วงร้อยละ 0 ถึง 7 โดยน้ำหนัก สำหรับประสิทธิภาพของเซลล์แสงอาทิตย์ชนิดสีย้อมไวแสงแบบใช้ไททาเนียเป็นอิเล็กโตรด พบว่าประสิทธิภาพของเซลล์อยู่ที่ 4.77±0.48% โดยผลของการเติมซีเรียมออกไซด์ทำให้ประสิทธิภาพของเซลล์ลดลง ในทางกลับกัน การเติมเซอร์โคเนียมออกไซด์และซิงค์ ออกไซด์ ทำให้ประสิทธิภาพของเซลล์เพิ่มขึ้นเป็น 6.57±0.26% และ 6.55±0.10% สำหรับการเติมเซอร์โคเนียมออกไซด์ ที่ร้อยละ 7 และการเติมซิงค์ออกไซด์ที่ร้อยละ 5 ตามลำดับ จากนั้นทำการศึกษาผลของชั้นฟิล์มอิเล็กโตรดแบบสองชั้นพบว่าให้การกระเจิงของแสงภายในอุปกรณ์ได้ดีกว่า ทำให้ประสิทธิภาพของเซลล์เพิ่มขึ้นจาก 6.57±0.26% เป็น 9.28±0.34% เมื่อเปรียบเทียบกับชั้นอิเล็กโตรดแบบชั้นเดียว

ภาควิชา วิศวกรรมเคมี ลายมือชื่อนิสิต .....

สาขาวิชา วิศวกรรมเคมี ลายมือชื่อ อ.ที่ปรึกษาวิทยานิพนธ์หลัก .....

ปีการศึกษา 2554

##5370523021: MAJOR CHEMICAL ENGINEERING
KEYWORDS: DYE-SENSITIZED SOLAR CELL/ SPRAY-COATED / TITANIA/ SOL-GEL

ANCHANA KITTITANESUAN: DYE-SENSITIZED SOLAR CELLS WITH TiO_2 ELECTRODE MODIFIED BY ZrO_2, CeO_2, OR ZnO. ADVISOR: AKAWAT SIRISUK, Ph.D. 62 pp.

This research investigated the application of ZrO_2/TiO_2, CeO_2/TiO_2 or ZnO/TiO_2 composite thin film as an electrode layer for a dye-sensitized solar cell (DSSC) and the effect on the fabrication of double-layer structure of the thin film electrode the performance of DSSC. Each metal oxide was individually synthesized via sol-gel methods and mixed before being sprayed onto the fluorine doped tin oxide (FTO) glass substrates using an ultrasonic spray coater. The electrode layer was fired at 400^oC for two hours. The amount of ZrO_2, CeO_2, or ZnO added to TiO_2 was varied from 0 to 10%wt (for ZrO_2) and 0 to 7% wt (for CeO_2, or ZnO). The DSSC with pure TiO_2 electrode layer had the efficiency of 4.77±0.48%. The addition of CeO_2 appeared to reduce the cell efficiency significantly. On the other hand, the addition of ZrO_2 or ZnO increased the amount of dye molecules adsorbed on the electrode surface, leading to improved short circuit current density (J_{SC}) and the efficiency of the cells when compared to cells with pure TiO_2 electrode. The highest cell efficiency of 6.57±0.26% and 6.55±0.10% were obtained for the DSSC with 7wt% ZrO_2/TiO_2 and 5wt% ZnO/TiO_2 electrode, respectively. Double-layer electrode (7wt% ZrO_2/TiO_2 on top of pure TiO_2) brought about better light scattering, thereby enhancing the overall energy conversion efficiency from 6.57±0.26% to 9.28±0.34% when compared with single-layered ZrO_2/TiO_2 electrode.

Department: Chemical Engineering Student's Signature .....

Field of Study: Chemical Engineering Advisor's Signature .....

Academic Year: 2011

ACKNOWLEDGEMENTS

This thesis would not have been possible to complete without the support of the following individuals. Firstly, she would like to express her greatest gratitude to her advisor, Dr. Akawat Sirisuk, for his invaluable guidance during the course of this work. And she is also very grateful to Professor Dr. Piyasan Praserthdam, for his kind supervision over this thesis as the chairman, Professor Dr. Suthichai Assabumrungrat and Dr. Nattaya Comsup, from Pathumwan Institute of Technology as the members of the thesis committee for their kind cooperation.

The author would like to acknowledge the financial support from Higher Education Research promotion and National Research University Project of Thailand, office of the Higher Education Commission.

Many thanks for kind suggestions and useful assistance from scientists at NECTEC for I-V tester measurement and many friends at the Center of Excellence on Catalysis and Catalytic Reaction Engineering, who always provide the encouragement and assistance along the study. To the many others, not specifically named, who have provided me with support and encouragement, please be assured that she thinks of them.

Finally, she also would like to dedicate this thesis to her parents and her brother, who have always been the source of her support and encouragement.

CONTENTS

PAGE

CHAPTER **PAGE**

CHAPTER **PAGE**

CHAPTER **PAGE**

LIST OF TABLES

TABLE **PAGE**

TABLE **PAGE**

TABLE **PAGE**

LIST OF FIGURES

FIGURE **PAGE**

FIGURE **PAGE**

CHAPTER I
INTRODUCTION

1.1. Rationale

Among the alternative energy resources such as biomass energy, wind energy, geothermal including solar energy, the solar energy has drawn much attention because of its low environmental impact. Therefore, the research on photovoltaic cell has attracted considerable interest. An example of such cell was the dye-sensitized solar cell (DSSC), which was proposed by O'Regan and Grätzel in 1991(O'Regan and Grätzel, 1991).

The DSSC is a device that directly converts sunlight into electrical energy. The DSSC has been continuously developed and there have been successive research reports on assembling DSSC in a sandwich structure. The DSSC consists of a transparent conducting glass, metal oxide film as an anode electrode, a dye sensitizer, a redox electrolyte, and a counter electrode. The metal oxide film such as TiO_2, ZnO (Wang et al., 2009), or SnO_2 (Bak wt al., 2011) have been used as an anode electrode. TiO_2, well known as a metal oxide semiconductor, has been studied extensively for many applications such as photocatalyst under ultraviolet light and dye-sensitized solar cells because TiO_2 has a wide band gap (3.2 eV for anatase and 3.0 eV for rutile). Moreover, TiO_2 can produce a higher overall efficiency than any other metal oxide and low cost production. The best DSSC efficiency with TiO_2 electrode is 11.2%, which was reported by Chiba et al., (Chiba et al., 2006).

Several attempts have been made to improve the properties of TiO_2 electrode, including modifying the structure of TiO_2, adding another metal oxide to increase surface area, fabricating a double layer structure with a good compactness to increase the dye adsorption (Chang et al., 2010), and including the second light scattering layer to increase light absorption (Han et al., 2009). In addition, there have been other attempts to develop the dye, electrolyte, or counter electrode (Yong et al., 2007).

This research focuses mainly on the improvement the power conversion efficiency of DSSC by modifying TiO_2 electrode. Another oxide, ZrO_2, CeO_2, or ZnO was mixed with TiO_2 sol for preparing thin film electrode. The double layer structure

was investigated including the effects of several preparation parameters on the cell efficiency.

1.2. Objectives

1. To enhance the efficiency of a dye-sensitized solar cells with TiO2 electrode modified by ZrO_2, CeO_2, or ZnO
2. To improve efficiency of a dye-sensitized solar cell by employing double-layer structure of the thin film electrode.

1.3. Research scopes

Part I

- Titanium dioxide (TiO_2), ZrO_2, CeO_2 and ZnO is prepared by sol-gel methods.
- The amount of ZrO_2, CeO_2 or ZnO added to TiO_2 is varied from 0 to 10%wt (for ZrO_2) and 0 to 7% wt (for CeO_2 and ZnO)**.**
- The mixed oxide electrode is characterized by several techniques.
    - X-ray diffractometry (XRD)
    - Nitrogen physisorption
    - UV-visible diffuse reflectance spectroscopy
    - Inductively coupled plasma optical emission spectrophotometer
- The efficiency of dye-sensitized solar cell is measured by an I-V tester.

Part II

- Study the effect of using double-layer thin film electrode that possesses similar specific surface area to that of a single-layer one.
- Characterize the electrode and the cell using several techniques already mentioned in Part I.

This thesis is arranged as follows:

Chapter I presented the introduction of this study.

Chapter II presented the structure and operation principles of dye-sensitizer solar cell (DSSC).

Chapter III presented the literature reviews of previous works related to this research.

Chapter IV presented the synthesis of the TiO_2 sol and modified TiO_2 by sol-gel methods, preparation of dye-sensitized solar cells and the fabrication procedure and characterization techniques used in this study.

Chapter V presented and discussed experimental results.

In the last chapter, Chapter VI presented overall conclusion and recommendations for the future studies.

CHAPTER II

THEORY

Dye-sensitized Solar Cell (DSSC)

The history of dye-sensitized solar cells (DSSC) started in 1972, which have been attracted much attention because of their low cost, easy to prepare and friendly to the environment. The DSSC offer a promising means of harvesting the sun's energy, and the improvement of their efficiency has drawn the interest of theoretical chemists and physicists.

The DSSC mainly consists of light sensitive dyes, porous layer of TiO_2 (wide band gap semiconductor), redox electrolyte, front and back electrodes made of transparent conducting oxide (FTO). At the heart of the system is a mesoporous oxide layer composed of nanometer-sized particles which have been sintered together to allow for electronic conduction to take place. The material of choice has been TiO_2 (anatase) although alternative wide band gap oxides such as ZnO and Nb_2O_5 have also been investigated.

2.1 Components and operation principles of DSSC

2.1.1 Titanium dioxide (TiO_2); Titania

Titanium dioxide (TiO_2) is an n-type wide band gap semiconductor (band gap 3.2 eV). TiO_2 has three main crystalline phases; anatase, which shows a higher a photocatalytic activity than the other types of Titania and is desirable for DSSC; rutile, which tends to be more stable at high temperatures; bookile, which is usually found only in minerals. Titania became the semiconductor of choice. The material has many advantages for sensitized photochemistry and photo-electrochemistry: it is a low cost, widely available, non-toxic, and biocompatible material (Grätzel, 2003).

There are several methods that can be used for synthesizing anatase Titania such as sol-gel methods, thermal decomposition method, precipitation method, and chemical vapor deposition. The difference of the preparation led to different of

surface area, pore sizes, and morphologies of the mesoporous films (Karthikeyan et al., 2006). Among of the different methods for the preparation of titania, sol-gel is mostly used because low cost, simplicity and large surface area.

The sol-gel conventional method uses the hydrolytic route, which involves the initial hydrolysis of the alkoxide precursor followed by continual condensations between the hydrolysed particles forming the gel. The hydrolysis and the polycondensation of titanium alkoxides proceed according to the following scheme (Harizanov et al., 2000):

$$\text{M-O-R} + H_2O \longrightarrow \text{M-OH} + \text{R-OH} \qquad \text{Hydrolysis reaction} \qquad (2.6)$$

$$\text{M-OH} + \text{HO-M} \longrightarrow \text{M-O-M} + H_2O \qquad \text{Water condensation} \qquad (2.7)$$

$$\text{M-O-R} + \text{HO-M} \longrightarrow \text{M-O-R} + \text{R-OH} \qquad \text{Alcohol condensation} \qquad (2.8)$$

Then, M substitute the semiconductor material sach as Si, Zr, Ti, Al, Sn or Ce
OR substitute the alkoxyl group

2.1.2 Counter electrode performance

Counter electrode (CE) is used to reduce the redox species oxidized at the working electrode, which act as a mediator in regenerating the sensitizer after electron injection in a liquid state DSSC. Several kinds of catalytic materials for CEs, such as platinum, carbon materials (graphite, activated carbon, carbon black, single-wall carbon nanotubes), poly(3,4-ethylenedioxythiophene) (PEDOT), poly(3,3-diethyl-3,4-dihydro-2H-thieno-[3,4-b][1,4]dioxepine) (PProDOTEt2), polypyrrole, and polyaniline have been introduced. Normally, platinum (Pt) is used for this layer due to its high catalytic property effect toward triiodide reaction, superior chemical and electrochemical stabilities. A thin layer of Pt nanoparticles is deposited on FTO by thermal decomposition, sputtering or electrochemical deposition (Hagfeldt, 2011 and Chen et al., 2010).

2.1.3 Dye-sensitized

Dye sensitizers serve as the solar energy absorber in DSSC, whose proprieties will have much effect on the light harvesting efficiency and the overall photoelectric conversion efficiency (Kong et al., 2007). The commercial of dyes widely used in DSSC have three types are N-3(Red dye), N-719(Black dye) and Z-907. Three dyes can be considered as the backbone of currently applied sensitizers in DSSC. All of these dyes are ruthenium based metal-organic complexes with the general formula $RuL_xL'_ySCN_z$, where L and L' are polypyridyl ligands; they are readily available commercially and show excellent efficiency levels up to 11%. The molecular structures of these dyes are shown in Figure 2.1. There is a widely used variant of the N-3 dye, which differs from it only in the degree of protonation (trivial name: N-719). The black dye shows the broadest absorption range up to 900 nm.

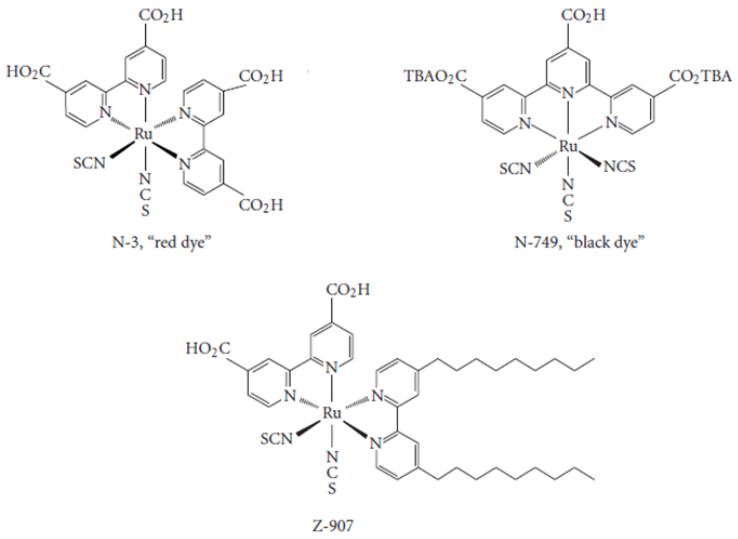

Figure 2.1 The tree most frequently applied ruthenium polypyridyl complexes (Lenzmann et al., 2007)

The amount of the sensitizer molecules available for light harvesting and charge injection are important upon adsorbing dye onto the metal oxide. Dye molecules are to be oriented on the surface of metal oxide with attachment functionalities of the molecule. Orientation reduces the covering area per adsorbed molecule, providing a more compact and packed arrangement of the dye molecules,

which allow for more adsorption dye of molecules. The rate constant for the migration of the excited energy would depend on the relative orientation of the donor and acceptor moieties. However, this is no longer possible if the dye is adsorbed as aggregates. Problem of poor electron transfer to the metal oxide conduction band would be arisen if dyes are aggregated that results in an unsuitable energetic position of the LUMO level. Lower current density could be resulted by poor injection efficiency, due to unfavourable binding of dye onto the metal oxide surface. The orientation of the molecule on the metal oxide surface is characterized by the anchoring group present in the dye (Rochford et al., 2007).

The fully protonated N3 has absorption maxima at 518 and 380 nm, the extinction coefficients being 1.3 and 1.33 × $10^4 M^{-1} cm^{-1}$, respectively. The optical transition has metal-to-ligand charge transfer (MLCT) character: excitation of the dye involves transfer of an electron from the metal to the p* orbital of the surface anchoring carboxylated bipyridyl ligand from where it is released within femto- to picoseconds into the conduction band of TiO_2 generating electric charges with unit quantum yield (Grätzel, 2003).

Moreover, dyes with enhanced molar absorption coefficients are attractive for efficient light harvesting with thinner TiO_2 layers. This can lead to an efficiency boost of DSSC concepts, which depends so far on such thin layers (particularly solid state- but also ionic liquid-based systems) and generally to improved V_{OC} independent of the type of system (Yong et al., 2007).

2.1.4 Electrolyte

The electrolyte is one of key components for dye-sensitized solar cells and its properties have much effect on the conversion efficiency and stability of the solar cells. The electrolyte used in DSSC is divided into three types: liquid electrolyte, quasi-solid, state electrolyte, and solid electrolyte. Liquid electrolyte could be divided into organic solvent electrolyte and ionic liquid electrolyte according to the solvent used.

One of the critical components of DSSC is the electrolyte containing a I^-/I_3^- redox couple that meditates the dye regeneration process. The contact of triiodide and semiconductor films (TiO_2) were restricted by the recombination between triiodide and electron in the conduction band of semiconductor. As the result, the fill factor and conversion efficiency of the solar cells were improved (Lee et al., 2011).

2.1.5 Operating principles

A standard solar cell uses the combination of P and N type semiconductors. The depletion region nearby the junction builds an electric field and the electrons in the region are driven from the N type to the P type. Fig. 2.2(a) describes the principle, where E_v, E_a, E_d, E_c are the energy band of conducting, acceptor, donor, and valence. Fig. 2.2(b) shows the schematic description of the electrons transformation for the DSSC.

The electrons of the DSSC emit and transfer arrange in the sequence as follows:

1. The dye (D) is excited (D*) by the absorption of photon energy (hν).

$$D + h\upsilon \rightarrow D^* \tag{1}$$

2. The electrons of excited dye jump to the conducting band (CB) of the TiO_2 at the same time.

$$D^* \rightarrow D^+ + e^-(CB) \tag{2}$$

3. The dye with emitted electrons (D^+) could react with the iodide ion (I^-) or receive the electrons from the conducting band of the TiO_2 and returns to the dye (D) again.

$$3I^- + 2D^+ \rightarrow I_3 + 2D \tag{3}$$

$$D^+ + e^- \rightarrow D \tag{4}$$

4. The iodide ion (I^-_3) further receives the electrons from the counter electrode and returns to the iodide ion (I^-) again.

$$I^-_3 + 2e^- \rightarrow 3I^- \quad (5)$$

The incident light is absorbed by the depletion region of the solar cell and its electrons jump from the P type to the N type, further emit from the N type to the external circle. In comparison with the DSSC shows the TiO_2 as the N type and the dye as the P type.

The photoelectric conversion efficiency (η) is defined as

$$\eta = \frac{Output\ Electric\ Power}{Input\ Solar\ Energy} \times 100\%$$

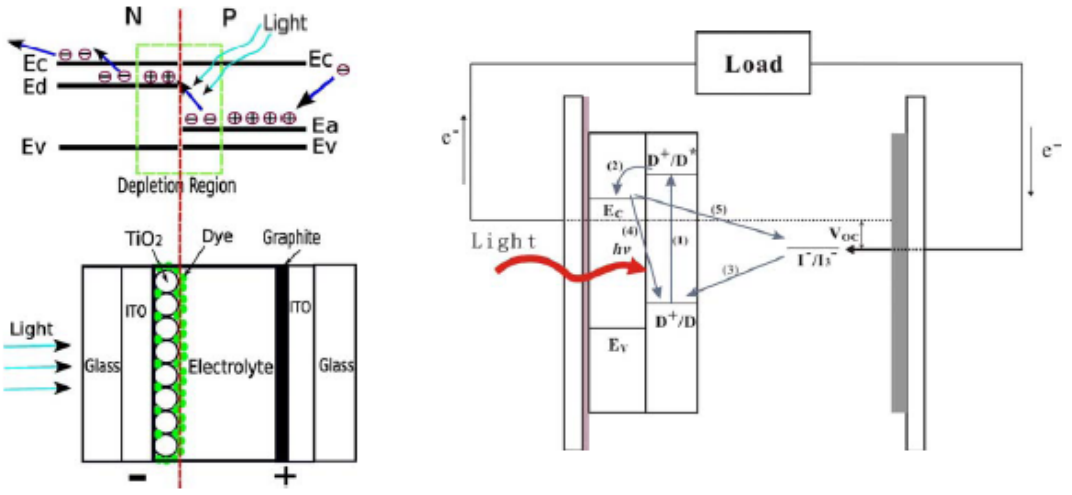

(a) Theoretical schema. (b) Schema of the electrons transformation.

Figure 2.2 Schematic description of DSSC (Chen et al., 2007)

2.2 Characteristics of the photovoltaic cell

The performance of each components is crucial and have been designated using the parameters: open-circuit voltage V_{oc}, fill factor FF and short circuit current density J_{sc} and expressed as efficiency (η) using the equation:

$$\eta = \frac{V_{OC} J_{SC} FF}{P_{in}}$$

and

$$FF = \frac{I_{max} V_{max}}{J_{sc} V_{OC}}$$

Whereas V_{oc}, is the maximum voltage obtained at zero current.

J_{sc}, the shot circuit current is the maximum current obtained under less resistance (short circuit) condition.

P_{in} is the solar radiation intensity.

I_{max} and V_{max} are the maximum current and maximum voltage, respectively.

CHAPTER III

LITERATURE REVIEWS

This chapter presents the literature reviews for dye-sensitized solar cell (DSSC).

3.1 Modification of TiO_2 electrode with mixed-metal oxides

Kim and coworkers (2009) investigated TiO_2 coated with various oxide layers; ZnO, SnO_2, ZrO_2, MgO, and Al_2O_3 electrode in DSSCs which fabricated by a screen printing method. They found that the open circuit voltage (V_{oc}) was closely dependent to the conduction band (CB) edge position and the band gap energy (E_g) of the oxide layers, while the short circuit current density (J_{sc}) depend on the dye adsorption and the iso-electric point (IEP).

MENZIES and coworkers (2004) prepared TiO_2 electrode, with some modified by successive deposition of ZrO_2 via sol-gel route and studied ZrO_2 shell formation on TiO_2 core nano particles. The result of ZrO_2-coated TiO_2 electrode to a higher efficiency to that of the uncoated TiO_2 electrodes. DSSC was constructed from the ZrO_2:TiO_2 core-shell electrode, the efficiency increased from 0.42% to 2.27%. But if the thickness of ZrO_2 shell increased, the cell efficiency was reduced.

Menzies and coworkers (2005) studied the precursor chemistry by comparing zirconium butoxide and zirconium isopropoxide. The results indicated that 0.05 M of zirconium butoxide coated on TiO_2 (P25 and anatase) electrodes, the cell efficiency increased more than using zirconium isopropoxide to be the precursor.

Kitiyanan and coworkers (2004-2005) studied the sole component of titania, zirconia and binary TiO_2–ZrO_2 oxides with various molar ratio of zirconia content from 5 mol% to 50 mol% were prepared by sol–gel methods of surfactant assisted mechanism. Moreover, the differential of calcinations was investigated. The addition of little amount of ZrO_2 increase the thermal stability of TiO_2 anatase phase as the transformation from the anatase phase to rutile phase of the TiZr5 at more than 800 ^oC

and completely transform to rutile phase at 1000 ^{o}C. The addition of a small amount of ZrO_2 did not change the structure of anatase-TiO_2. In addition, The advantages of using the binary oxide as an electrode of dye-sensitized solar cells are the increase of BET surface area which leads to the increase of J_{sc} and the increase optical band gap which leads to the increase of V_{oc}. These increases enhanced the solar energy conversion efficiency.

Kim and coworkers (2004) investigated the surface of the TiO_2 nanoparticles with modified by ZnO coated TiO_2 nanoparticles. To provide an inherent energy barrier between the electrode and electrolyte interface led to a reduced recombination of photoinduced electrons. In addition, the value of J_{sc}, V_{oc}, the fill factor, and overall conversion efficiency were increased from 0.35 to 0.49 mA/cm^2, from −0.67 to −0.72V, from 61.1 to 69.0%, and from 0.71 to 1.21%, respectively.

Kao and coworkers (2009) preparation ZnO-coated TiO_2 (ZTO) thin films were deposited on ITO substrates by a sol–gel method. ZnO-coated TiO_2 thin films were studied and compared single TiO_2 film. The results that the BET surface area and amounts of adsorbed dye of the pure TiO_2 thin film and the ZTO thin films were almost the same. The values of J_{sc} and V_{oc} were improved and can be explained by the suppression of interfacial charge recombination due to ZnO coating, resulting in an increase in conversion efficiency as well as fill factor compared to the single TiO_2 thin film.

Shanmugam and coworkers (2010) studied the electron transport and recombination in DSSC with TiO_2/ZnO core-shell photoelectrode. The formation of ZnO shell on TiO_2 nanoparticles can effectively prevent the electron back reaction from the conduction band of the mesoporous TiO_2 to the surface states and eventually suppressed the recombination of the photoexcited electrons with either a hole available in electrolyte or oxidized dye molecules and hence the reduced processes 2, 3, and 4 in figure 3.1. In addition, Process1 shows the electron injection from the LUMO of the dye to the E_C of TiO_2, process2 from the E_C to active surface states which are close to the redox potential of the electrolyte before transferred to the

indium tin oxide (ITO) electrode. Now, the trapped electron by the surface states has two recombination probabilities which are recombination either with oxidized dye molecule, process3 or with electrolyte, process4.

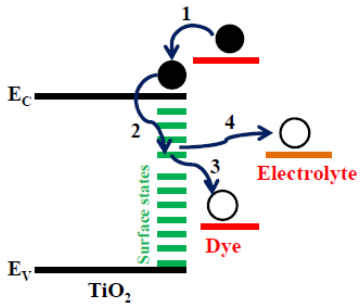

Figure 3.1 Electron transport and recombination pathways in DSSC (Shanmugam et al., 2010)

Chou and coworkers (2012) investigated the applicability of a ZnO-coated TiO_2 working electrode in a dye-sensitized solar cell (DSSC). The ZnO coated TiO_2 to improve the open-circuit voltage and the power conversion efficiency of a DSSC and to retard any back reaction. This result is probably attributed to the following facts.(1) An energy barrier is constructed by coating ZnO on the TiO_2 (P-25) film because the potential level of the CB of ZnO (−0.15 eV) is higher than that of the CB of TiO_2 (−0.1 eV); (2) this energy barrier may suppress the charge recombination and decrease the dark current generated in a DSSC, and its schematic is shown in Fig. 6, which indicated that raising the energy level of the metal oxide conduction band should reduce the recombination losses and result in high open circuit voltage; (3) the open-circuit photovoltage is increased due to the negative shift (toward vacuum level) of the Fermi-level of ZnO-coated TiO_2; and the higher the recombination of conduction band electrons with the electrolyte, the lower will be the FF.

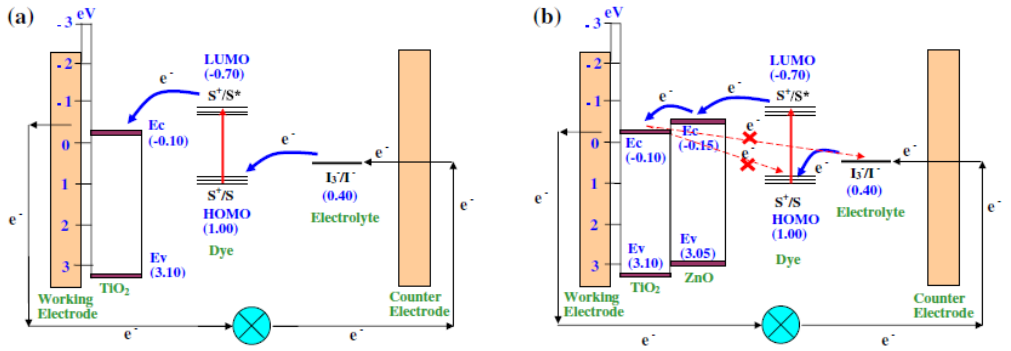

Figure 3.2 Schematic of the mechanism of the DSSC. (a) The conventional DSSC, (b) the DSSC with a ZnO barrier (Chou et al., 2012).

3.2 The structure of TiO_2 electrode of the dye-sensitized solar cell

Xu and coworkers (2010) prepared bilayer-structured film with TiO_2 nanocrystals as underlayer and TiO_2 nanotubes as overlayer onto FTO glass using doctor-blade technique. The results indicated that double-layer TiO_2 film could significantly improve the efficiency of DSSC. The effect of the bilayer structure on photovoltaic performance of cells was investigated. The effective dye adsorption and rapid electron transport of double-layer TiO_2 cell enhanced solar cell performance and J_{sc}. The value of solar cell performance and J_{sc} is 6.15% and 14.3mA/cm^2, respectively. The charge recombination behavior of cells was investigated by electrochemical impedance spectra, and the results showed that double-layer TiO_2 film-based cell possessed the lowest transfer resistance and the longest electron lifetime.

Chang and coworkers (2009) prepared multilayer-type TiO_2 film by coating TiO_2 nanoparticle Degussa P25 on indium tin oxide (ITO) glass substrate. The multilayer-type TiO_2 film can increase the dye adsorption capability of the thin film including multilayer is a good compactness of film compared with single-layer TiO_2 thin film. The I-V curve of the produced DSSC shows that it has an excellent energy conversion efficiency of 6.9%.

Wang and coworkers (2004) designed and investigated TiO_2 photoelectrodes with six different structures (see in Figure 3.3), with layers of nanoparticles, light-scattering particles, and mixture of nanoparticles and light-scattering particles on the conducting glass at a desirable sequence and thickness. They found that increasing surface area and light scattering could not simultaneously because they oppose each other. Therefore, there must be a balance between them. The cell performance depends on the film morphology for a given DSSC. The solar energy conversion efficiency has been improved significantly from 7.6 to 9.8% by tuning the film structure from monolayer to multilayer. The best efficiency of 10.2% under illumination of simulated AM1.5 solar light was attained with a multilayer structure using an anti-reflection film on the cell surface.

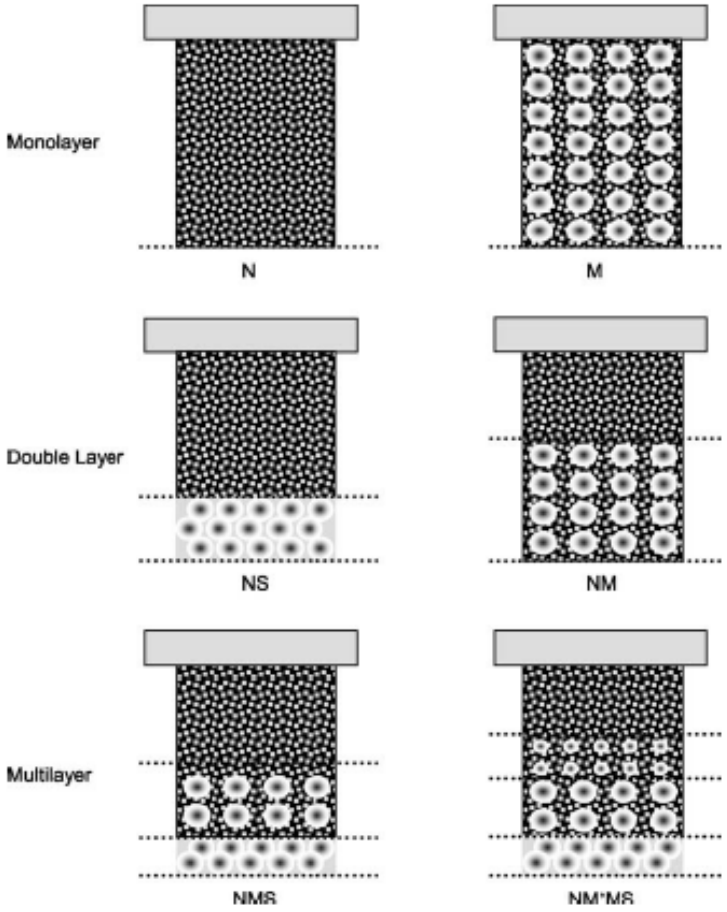

Figure 3.3 Schematic film morphologies of studied TiO_2 photoelectrodes. (Wang et al., 2004)

CHAPTER IV

EXPERIMENTAL

This chapter discusses various material and method employed in this research. The experiments involved (i) preparation of TiO_2 film and metal oxide dope TiO_2 film, and measuring their characteristics. (ii) preparation of dye-sensitized solar cell components. (iii) assembled the DSSC by fit: the working electrode, the counter electrode and the electrolyte, and (iv) physical and electrochemical characterization.

4.1 Preparation of TiO_2 film and metal oxide dope TiO_2 film

The preparation of the TiO_2 film and metal oxide dope TiO_2 film consisted of two steps: the preparation of TiO_2 sol via sol gel method and the application of TiO_2 sol onto electrode by ultrasonic spray coating.

4.1.1 Preparation of TiO_2 sol

TiO_2 sol was prepared via a sol-gel method. A solution consisted of 7.51 ml of 65% nitric acid and 1000 ml of distilled water. Titanium (IV) isopropoxide (TTIP) in the amount of 83.40 ml was added slowly into the solution while being strirred continuously at room temperature. The mixture solution was stirred for 3-4 days until clear sol was obtained. Next, the clear sol underwent dialysis in a cellulose membrane. The distilled water used for dialysis was changed daily until a pH of 3.5 was obtained. And then, TiO_2 sol was kept in a refrigerator until needed.

4.1.2 Preparation of metal oxide dope TiO_2 sol

In this work , another oxide was added to TiO_2 film. The metal oxide chosen for this study were ZrO_2, CeO_2, and ZnO, which were added to a TiO_2 sol at concentrations of 1.0%, 3%, 5% , and 7.0% (w/w).

4.1.2.1 Preparation of ZrO_2/TiO_2 sol

To prepare ZrO_2 sol, one mixed 2.2 ml of 70% HNO_3 in 105.2 ml of deionized water and zirconium butoxide in the amount of 7.6 ml was added slowly into the

solution while being strirred continuously at room temperature. The mixture solution was stirred for 2-3 days until clean and homogeneous sol was obtained.

To obtain 1.0%, 3%, 5%, and 7.0% (w/w) of ZrO_2/TiO_2 mixture, one mixed 0.72 ml, 2.15 ml, 3.59 ml and 5.03 ml of ZrO_2 sol, respectively, with 79.84 ml, 78.23 ml, 76.61 ml, and 75.00 ml of TiO_2 sol, respectively. The solution was stirred until homogeneity was obtained. Then, the mixture solution underwent dialysis in a cellulose membrane until a pH of 3.5 was obtained.

4.1.2.2 Preparation of CeO_2/TiO_2 sol

CeO_2 sol prepared by dissolving 0.5 g of $Ce(NO_3)_3 \cdot 6H_2O$ in 25 ml of distilled water while being stirred continuously until homogeneous solution, after its pH value was adjust to about 2 by using 5M of nitric acid solution.

To obtain 1.0%, 3%, 5%, and 7.0% (w/w) of CeO_2/TiO_2 mixture, one mixed 4.83 ml, 19.32 ml, 24.15 ml and 33.81 ml of ZrO_2 sol, respectively, with 86.84 ml, 85.09 ml, 83.34 ml, and 81.58 ml of TiO_2 sol, respectively. The solution was stirred until homogeneity was obtained. Then, the mixture solution underwent dialysis in a cellulose membrane until a pH of 3.5 was obtained.

4.1.2.3 Preparation of ZnO/TiO_2 sol

Zinc oxide was prepared by dissolving of $C_4H_6O_4Zn \cdot 2H_2O$ in distilled water. To obtain 1.0%, 3%, 5%, and 7.0% (w/w) of ZnO/TiO_2 mixture, one dissolving 0.0450 g, 0.04593 g, 0.04690 g and 0.04791 g of ZnO sol, respectively in distilled water and mixed with 79.84 ml of TiO_2 sol. The solution was stirred until homogeneity was obtained.

4.2 Preparation of dye-sensitized solar cell components and the fabrication procedure

The components of DSSC are mainly considered of transparent conducting glass, dye, electrolyte, counter electrode and anode electrode.

4.2.1 Transparent conducting oxide glass

The conducting glass is transparent conducting oxide coated glass, which is the fluorine-doped tin oxide (FTO) coated on electrically conducting glass. The glass was purchased from Solaronix (Switzerland) under the commercial name TCO22-15. To identify the conducting side of fluorine doped tin oxide coated on glass, one used a multimeter to measure resistance. The conducting side would have a sheet resistance of ca. 15-20 ohm. The glass was cleaned with ethanol and dried with a hair-dryer.

4.2.2 Dye sensitized

In this research, this work employed Cis-di(thiocyanate)bis(2,2'-bipyridine-4,4'-dicarboxylate)ruthenium (II) or N3 (R535) dye from Solaronix, which was widely used in dye-sensitized solar cell. To prepare the dye solution, 20 mg of N3 dye was dissolved in 100 ml of ethanol and the mixture was stirred until a homogeneous solution was obtained. The resulting product was a solution of 0.3 mM N3 dye in ethanol.

4.2.3 Electrolyte

Electrolyte consisted of 0.5 M lithium iodine (LiI), 0.05 M iodide (I_2), and 0.5 M 4-tert-butylpyridine (TBP) in acetronitrile, one mixed 2.00 g of LiI, 0.38 g of I_2, and 2.20 ml of TBP in 30 ml of acetronitrile. The solution was stirred until homogeneity was obtained.

4.2.4 Counter electrode

The counter electrode for the DSSC was platinum coated on conducting glass. To prepare a platinum counter electrode by ion sputtering, one first cut a conducting glass to a rectangular piece that was 1.0×1.5 cm^2 in site. The glass was cleaned with ethanol was dried with a hair-dryer. Then, tape was placed on one side of the glass as seen in Figure 4.1. Wipe off any fingerprints using a tissue wet with ethanol. Then, platinum target was sputtering on the conducting glass using ion sputtering (JEOL JFC-1100E) at 10 mA of ion current for four minutes. After sputtering, masking tape was removed.

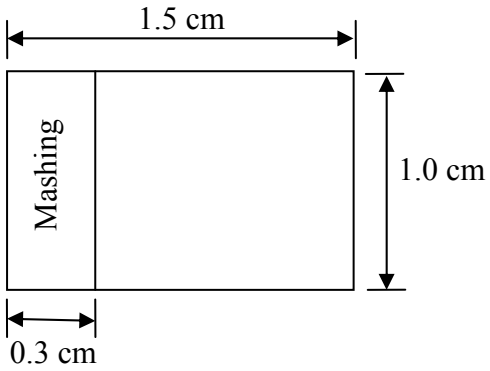

Figure 4.1 The counter electrode before sputtering

4.2.5 Anode electrode

Anode electrode consisted of TiO_2 film or metal oxide dope TiO_2 film on a conducting glass. To prepare the anode electrode, first we cut a conducting glass into a rectangular piece that was 1.0×1.5 cm^2. The glass clean with ethanol and dry with a hair-dryer. Then the glass was masked with aluminum foil to a circle have radius 0.5 cm as seen in Figure 4.2. The cut out was located closer to one side of the foil than the other.

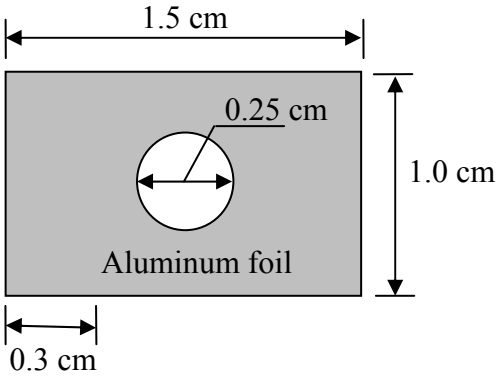

Figure 4.2 The anode electrode before spray coating

After masking, TiO_2 was coated on the conducting glass using ultrasonic spray coater. Stir well the TiO_2 sol before use, not shake unless bubbles could be formed. The spraying liquid such as TiO_2 sol was placed in a syringe pump, which fed the liquid at a rate 1 ml/min to an ultrasonic nozzle. The level speed of a moving stage

was 4. The power of an ultrasonic nozzle, provided by a frequency generator until was 3.5 watts.

This study effect of modified TiO_2 electrode then this work controlled the number of coats of TiO_2 sol, ZrO_2/TiO_2 sol, CeO_2/TiO_2 sol or ZnO/TiO_2 sol at 500 coats. After a few coats, TiO_2 thin film was dried by a hair dryer. The thickness of film was measured using profilmeter (Veeco Dektak 150). The anode electrode was sintered at 400°C for two hours. After anode electrodes was left to be cooled to 30°C. Before dye impregnation, we heat electrode on hotplate at 70°C for 10 minute, to avoid water absorption. Put slowly the anode electrode was immersed in a solution of 0.3 mM N3 dye for 24 hours in the dark. Then, the anode electrode rinsed with ethanol (The ethanol remove water from the porous TiO_2) and dye with hair-dryer. Finally, the anode electrodes were assembled.

4.3 Assembled and texted the DSSC

Assembly the two electrodes (counter and anode electrode), First this work cut two strips of a sealing material that were 0.15 cm wide and 1.2 cm long. The strips were inserted as spacer between the platinum counter electrode and anode electrode. The platinum counter electrode was placed on top of the anode electrode so that the conducting side of the counter electrode was on top of the TiO_2 film. The cell was sealed by heating the sealing material with a hotplate at 60°C for 3 minute (see Figure 4.3)

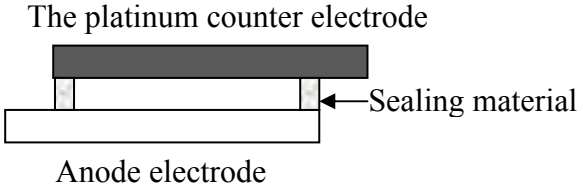

Figure 4.3 Cross-section of assembled dye solar cell showing sealing rim

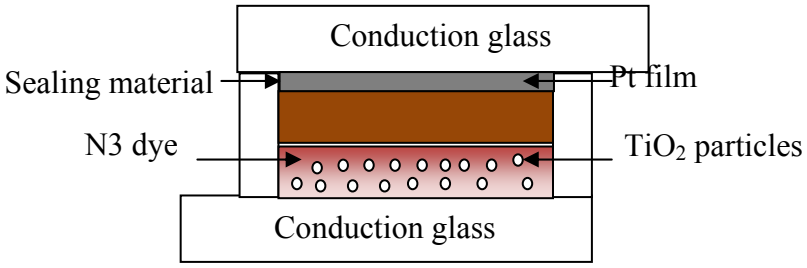

Figure 4.4 Fabrication of dye-sensitized solar cell assembly for testing

For electrolyte filling, in cell having a sealing rim with two small holes, the filling is done by putting a droplet onto only one hole, and let it soak up (see Figure 4.4), then clean carefully the area around the filling holes with acetone. The cell is ready for testing.

4.4 Physical and electrochemical characterization

In this section discussed various techniques for physical and electrochemical properties of TiO_2, metal oxide dope TiO_2 and dye sensitized, various characterization techniques were employed.

4.4.1 X-ray diffractometry (XRD)

XRD was performed to determine crystal phase and crystallite size of TiO_2, ZrO_2/TiO_2, CeO_2/TiO_2 and ZnO/TiO_2. It was conducted using a SIEMENS D5000 X-ray diffractometer with Cu Kα radiation (λ= 1.54439Å) with Ni filter. The spectra were scanned at a rate of 0.04 min-1 in the 2θ range of 20-80^o.

4.4.2 Nitrogen physisorption

To determine the specific surface area of TiO_2, ZrO_2/TiO_2, CeO_2/TiO_2 and ZnO/TiO_2 were measured through nitrogen gas adsorption in a continuous flow method at liquid nitrogen temperature. A mixture of nitrogen and helium was employed as the carrier gas using Micromeritics ChemiSorb 2750 Pulse Chemisorption Ststem instrument. The sample was thermally treated at 200°C for one hour before measurement.

4.4.3 UV-Visible absorption spectroscopy (UV-Vis)

To determine the amount of dye adsorption was determine by a spectroscopic method by measuring the concentration of dye desorbed on the titania film into a mixed solution of 0.1M NaOH and ethanol (1:1 in volume fraction). The absorption spectra by UV-Vis Absorption Spectroscopy (Perkin Elmer Lampda 650, λ between 300-800 nm and step size 1 nm).

To study the light absorption behavior of the catalysts, the absorbance spectra of the catalysts in the wavelength range of 200-800 nm were obtained using a Perkin Elmer Lambda 650 spectrophotometer. The step size for the scan was 1 nm. The band gap (E_g) of the sample was determined by the following equation (4.1):

$$E_g = \frac{1240}{\lambda} \tag{4.1}$$

Where E_g is the band gap (eV) of the sample, λ (nm) is the wavelength of the onset of the spectrum.

4.4.4 Inductively Coupled Plasma-Atomic Emission Spectroscopy (ICP-AES)

The amount of metal deposited on the surface of titanium dioxide (TiO_2) was measured with an Optima 2100 DV spectrometer. The sample was solution, we dissolved 0.01 g of catalyst in 5 ml of 49% hydrofluoric acid (Merck) stirred until homogenous solution then the solution make to 100 ml with deionized water. The solution has concentration of 5 ppm (mg·l-1) from the catalyst which was assumed to have metal content of 2.0 wt %.

4.4.5 Current-Voltage Tester (I-V Tester)

The electrochemical properties of dye-sensitized solar cell were determined by I-V tester Current-Voltage measurements were performed using white light source under air mass (AM) 1.5G condition. To determine current density, open circuit voltage, cell resistance, and fill factor. This information was then converted to efficiency of the solar cell. An area of our solar cell was 0.196 cm^2. The equipment used was MV systems Inc., Xenon short ARC (Osram XBO 1000 W/HS).

CHAPTER V

RESULTS AND DISCUSSION

This chapter presents the experimental results and discussion on effect of addition of the ZrO_2, CeO_2 and ZnO to TiO_2 electrode layer includes described influence of double-layer structure of the thin film electrode on the performance of dye-sensitized solar cell.

5.1 Effect of modification of TiO_2 electrode layer

5.1.1 Modification of TiO_2 electrode layer by addition ZrO_2

TiO_2 was prepared via sol-gel method. It has been used as an electrode in DSSC. TiO_2 electrode layer was modified by ZrO_2 to electrode at the percentage of ZrO_2/TiO_2 was 1.0%wt, 3.0%wt, 5.0%wt and 7.0%wt. The ZrO_2/TiO_2 was spray-coated on FTO glass substrates 500 times. The electrode layer was calcined at 400^oC for two hours. This work studied influence of the addition of ZrO_2 with the performance of dye-sensitized solar cells which control sintering temperature and thickness of film.

X-ray diffraction (XRD) patterns for the pure TiO_2 and ZrO_2/TiO_2 composite are shown in Figure 5.1. The XRD peaks at 2θ values of 25.32^o, 37.88^o, 48.16^o and 62.80^o corresponded to the anatase phase, whereas the XRD peaks at 2θ values of 27.44 ^{o}, 41.28 ^{o} and 54.36^o corresponded to rutile phase and the XRD peak at 2θ values of 30.88^o corresponded to brookite phase (Porkodi and Arokiamary, 2007). All samples consisted of antase phase as the major phase and small amounts of rutile and brookite phase. The average crystalline size can be calculated from the width at half-height of the diffraction peak of XRD pattern using the Debye-Scherrer's equation equation is listed in Table 5.1. It has been indicated that anatase phase has higher photocatalytic oxidation-reduction activity than rutile phase. The band gap energies for anatase phase and rutile phase have been estimated to be 3.2 and 3.0 eV, respectively (Chen et al., 2010).

Table 5.1 reported specific surface area of TiO_2 and ZrO_2/TiO_2 powders measured by single point adsorption from nitrogen physicsorption technique includes reported crystallite size and weight fraction of anatase, rutie and brookite phase. The weight fraction of anatase of TiO_2 increases with increasing of percentage of ZrO_2 while the crystallite sizes decreases with increasing of percentage of ZrO_2. The added ZrO_2 role was based on the crystal growth inhibiter, which leading to small grain size correlated with increasing surface area.

In addition, inductively coupled plasma atomic emission spectroscopy (ICP-AES) was used to consider the amount of Zr on Ti catalyst. The results of ICP analysis found that the contents of Zr less than the nominal value may because the preparation of mixed oxide sol.

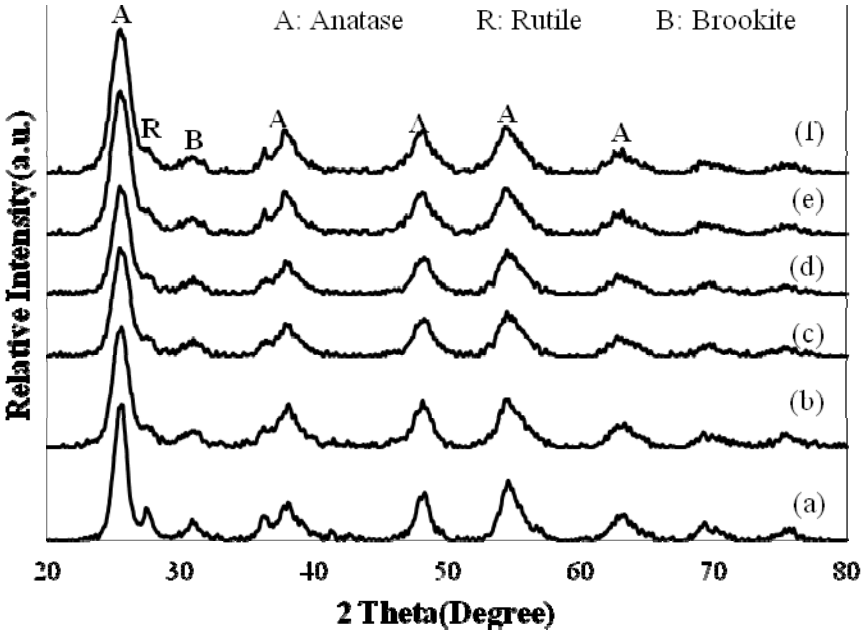

Figure 5.1 XRD patterns of ZrO_2/TiO_2 powders at various percentages of ZrO_2 (a) 0 wt %, (b) 1.0 wt %, (c) 3.0 wt % (d) 5.0 wt % (e) 7.0 wt % and (f) 10.0 wt %

Table 5.1 Crystalline size, surface area and weight fraction of anatase, rutile and brookite of ZrO_2/TiO_2 powders calcined at 400°C for 2 hours

Zr/Ti (wt%)	Crystallite size (nm)	Surface area (m^2/g)	Amount of Zr from ICP (wt%)	W_A	W_R	W_B
Pure TiO_2	6.3	77	-	0.55	0.16	0.28
1.0	5.2	102	0.96	0.61	0.11	0.26
3.0	4.9	97	2.94	0.63	0.14	0.23
5.0	4.7	109	4.25	0.63	0.12	0.25
7.0	4.6	115	6.39	0.64	0.11	0.24
10.0	3.7	120	9.71	0.62	0.19	0.28

W_A: weight fraction of anatase phase

W_R: weight fraction of rutile phase

W_B: weight fraction of brookite phase

Table 5.2 and Figure 5.2 shows the UV-visible light absorption characteristics for pure TiO_2 and ZrO_2/TiO_2. There could analyze transfer of electron-hole pairs in semiconductor particle and determine the amount of N3 dye adsorbed on TiO_2 and ZrO_2/TiO_2 electrodes, respectively.

The results of the addition of ZrO_2 had wide band gap when compare with pure TiO_2. The ZrO_2/TiO_2 7%wt could be activated under UV range (less 400 nm) as well. Therefore, the ZrO_2/TiO_2 7%wt electrode didn't block the adsorption of N3 dye. In addition, the N3 dye will be work as well if semiconductor didn't adsorb light in visible range (400-800 nm). The intrinsic band gap absorption of TiO_2 was 3.2 eV (388 nm) for anatase phase and 3.0 eV (420 nm) for rutile phase (Amornpitoksuk and Leesakul, 2003). It can be concluded that the weight fraction of anatase phase enhanced with increasing the contents of ZrO_2 modification which effect to increasing of band gap (see in Table 5.1).

Table 5.2 The comparison band gap from UV-vis spectra of titanium dioxide doped with various amount of Zerconia calcined at 400°C for 2 hours.

Sample	Wavelength (nm)	Band gap energy (eV)
Pure TiO_2	415	3.00
ZrO_2/TiO_2 1.0%wt	412	3.02
ZrO_2/TiO_2 3.0%wt	401	3.10
ZrO_2/TiO_2 5.0%wt	400	3.11
ZrO_2/TiO_2 7.0%wt	397	3.13
ZrO_2/TiO_2 10.0%wt	400	3.11

Moreover, the amount of dye adsorbed on the TiO_2 and ZrO_2/TiO_2 electrodes were determined by dissolving the dye from the electrode with a mixed solution of 0.1M NaOH and ethanol at a volume ratio 1:1. The dye solution was then analyzed by UV-Visible spectrophotometer to determine the concentration. The amount of dye adsorbed on the TiO_2 and ZrO_2/TiO_2 electrodes are presented in Figure 5.2. The amount of dye adsorption increased when the ZrO_2 content increased, compared with pure TiO_2 electrode. The increasing of content ZrO_2 led to enhance of light harvesting and increase short circuit photocurrent for DSSCs. It can be concluded that the adsorption of N3 dye increased correspond with increasing of surface area. In the addition, the wavelength of laser was selected as 510 nm because the dye molecules have maximum adsorption around this wavelength.

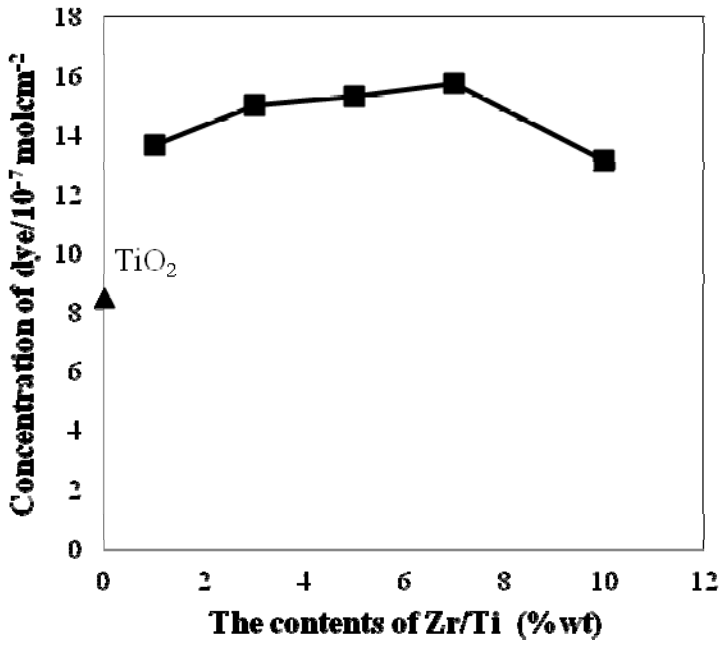

Figure 5.2 Relationship between concentrations of dye with various contents of ZrO_2/TiO_2

The TiO_2 and ZrO_2/TiO_2 electrodes layer were prepared by ultrasonic spray coating on FTO substrate. The electrode layer was sintered at 400^oC for two hours. The amount of ZrO_2 was varied from 0 to 7% (w/w). The photovoltaic properties were measured by the I-V tester under AM 1.5 irradiation. The observed I-V characteristics was tabulated in the Table 5.3 the corresponding solar cell parameters**.** For pure TiO_2 electrode layer produced the efficiency of 4.77±0.48%. Modification of TiO_2 electrode with ZrO_2 gave rise to higher cell efficiency. The highest cell efficiency of 6.57±0.26% was obtained with a DSSC with 7wt% ZrO_2/TiO_2 electrode. The current density enhanced from 7.90±0.80 to 8.48±0.57mA·cm^{-2} for 7wt% of ZrO_2/TiO_2 electrode compare with pure TiO_2 electrode. This was in agreement the amount of dye adsorbed on the surface of the electrode (see Figure 5.2). When the content of ZrO_2 was increased to 10.0 wt %, the amount of the dye adsorbed shows decrease with the increase of ZrO_2 content, which will result in the decrease of the light harvesting efficiency.

Table 5.3 Electrochemical properties of dye-sensitized solar cell of ZrO_2/TiO_2 electrode calcined at 400°C for 2 hours with 500 coats

ZrO_2/TiO_2 (wt%)	V_{OC} (Volt)	J_{SC} ($mA \cdot cm^{-2}$)	Fill Factor	Efficiency (%)
Pure TiO_2	0.74±0.01	7.90±0.80	0.81±0.06	4.77±0.48
1.0	0.71±0.04	7.35±1.16	0.99±0.06	5.08±0.58
3.0	0.70±0.03	9.51±0.40	0.86±0.06	5.71±0.31
5.0	0.74±0.01	7.19±0.90	1.08±0.09	5.63±0.19
7.0	0.74±0.00	8.48±0.57	1.05±0.06	6.57±0.26
10.0	0.75±0.01	6.03±1.06	0.99±0.09	4.45±0.76

5.1.2 Modification of TiO_2 electrode layer by addition CeO_2

TiO_2 electrode layer was modified by CeO_2 to electrode at the percentage of CeO_2/TiO_2 was 1.0%wt, 3.0%wt, 5.0%wt and 7.0%wt. The CeO_2/TiO_2 was spray-coated on FTO glass substrates 500 times. The electrode layer was calcined at 400^{o}C for two hours.

Figure 5.3 shows the XRD patterns of the phase structure of the pure TiO_2 and CeO_2/TiO_2 composite. The results of XRD patterns showed that the addition of CeO_2 inhibited the phase transformation of TiO_2 from anatase to rutile up to 3 wt% of CeO_2/TiO_2 which it was decrease slightly with the content of CeO_2 increase (see in Table 5.4).

Table 5.4 reported the various contents of Ce on Ti catalyst from ICP analysis. From result of ICP analysis found that the contents of cerium more than the nominal value may because the preparation of mixed oxide sol. Moreover, this table showed that the crystallite size and surface area which The CeO_2/TO_2 had higher surface area than pure TiO_2.

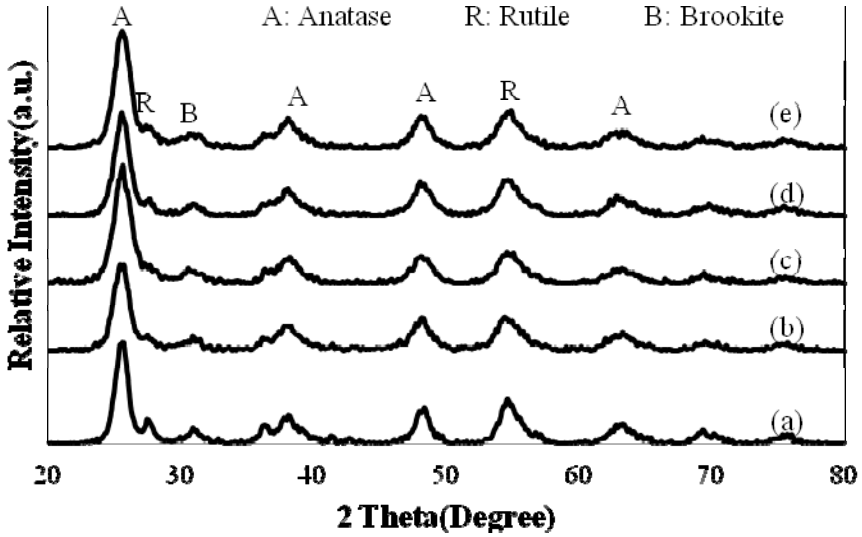

Figure 5.3 XRD patterns of CeO_2/TiO_2 powders at various percentages of CeO_2 (a) 0 wt %, (b) 1.0 wt %, (c) 3.0 wt % (d) 5.0 wt % and (e) 7.0 wt %

Table 5.4 Crystalline size, surface area and weight fraction of anatase, rutile and brookite of CeO_2/TiO_2 powders calcined at 400°C for 2 hours

Ce/Ti (wt%)	Crystallite size (nm)	Surface area (m^2/g)	Amount of Zr from ICP (wt%)	W_A	W_R	W_B
Pure TiO_2	6.3	77	-	0.55	0.16	0.28
1.0	5.3	83	1.34	0.57	0.12	0.31
3.0	5.0	114	3.01	0.57	0.17	0.24
5.0	5.1	105	5.12	0.47	0.19	0.34
7.0	3.3	113	7.09	0.41	0.21	0.38

Figure 5.4 showed the amount of the adsorbed dye on TiO_2 and CeO_2/TiO_2 electrode. Generally, the amount of dye adsorbed on TiO_2 and CeO_2/TiO_2 electrode will related with the specific surface area of electrode. It can be observed that the amount of the adsorbed dye decreases with the increase of the CeO_2 content, while its

specific surface area increase when compared with pure TiO_2. Therefore the specific surface area was not mainly responsible for the decrease of the dye adsorption.

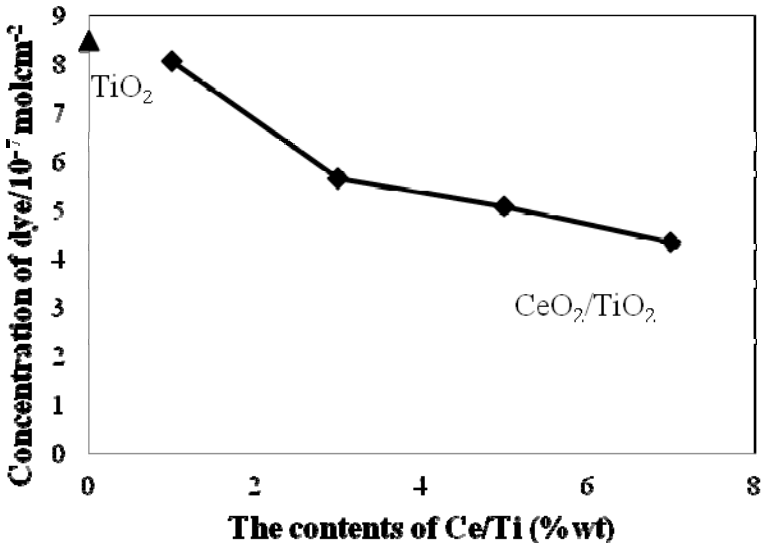

Figure 5.4 Relationship between concentrations of dye with various contents of CeO_2/TiO_2

The transfer of electron-hole pairs in semiconductor particle was analyzed by UV-visible absorption spectroscopy. The results showed that the addition of CeO_2 reduced band gap when compare with pure TiO_2. The energy band gap of CeO_2/TiO_2 decreased with increasing of content of CeO_2 (see in Table 5.5). The addition of CeO_2 gave rise to a new absorption appears at around 480 to 500 nm. The CeO_2/TiO_2 could be activated under visible range (400-800 nm) as well. Therefore, the CeO_2/TiO_2 electrode may be blocked the light adsorption of dye which will part of decreasing of the light harvesting efficiency.

Table 5.5 The comparison band gap from UV-vis spectra of titanium dioxide doped with various amount of Ceria calcined at 400°C for 2 hours.

Sample	Wavelength (nm)	Band gap energy (eV)
Pure TiO_2	415	3.00
CeO_2/TiO_2 1.0%wt	480	2.59
CeO_2/TiO_2 3.0%wt	500	2.49
CeO_2/TiO_2 5.0%wt	503	2.47
CeO_2/TiO_2 7.0%wt	504	2.46

The observed I-V characteristics was tabulated in the Table 5.6 the corresponding solar cell parameters**.** The CeO_2/TiO_2 electrode calcined at 400 ^oC for two hours by various the content of cerium. The CeO_2 was added to TiO_2 electrode, the cell efficiency dropped significantly when the cerium content exceeded 3 wt% (see in Table 5.6). This could be attributed to lower amount of dye adsorption when CeO_2 was added to TiO_2 electrode (see Figure 5.4). The photocurrent density decreased as a function of cerium content, which confirmed the previous discussion about the dye adsorption effect of CeO_2 modification

Table 5.6 Electrochemical properties of dye-sensitized solar cell of CeO_2/TiO_2 electrode calcined at 400°C for 2 hours with 500 coats

CeO_2/TiO_2 (wt%)	V_{OC} (Volt)	J_{SC} ($mA \cdot cm^{-2}$)	Fill Factor	Efficiency (%)
Pure TiO_2	0.74±0.01	7.90±0.80	0.81±0.06	4.77±0.48
1.0	0.70±0.01	6.17±0.13	0.90±0.06	3.87±0.21
3.0	0.60±0.03	0.52±0.04	0.50±0.06	0.16±0.03
5.0	0.52±0.01	0.44±0.01	0.43±0.03	0.10±0.01
7.0	0.49±0.01	0.43±0.06	0.35±0.02	0.07±0.01

5.1.3 Modification of TiO2 electrode layer by addition ZnO

TiO_2 electrode layer was modified by ZnO to electrode at the percentage of ZnO/TiO_2 was 1.0%wt, 3.0%wt, 5.0%wt and 7.0%wt. The ZnO/TiO_2 was spray-coated on FTO glass substrates 500 times. The electrode layer was calcined at 400^{o}C for two hours.

Figure 5.5 shows XRD patterns of the phase structure of the pure TiO_2 and ZnO/TiO_2 powder at various content of ZnO add to TiO_2. The results of XRD patterns showed that anatase phase as the major phase and small amounts of rutile and brookite phase. The average crystallite size of ZnO/TiO_2 was listed in Table 5.7 includes specific surface area and weight fraction of anatase, rutile, and brookite phase. The crystallite size of ZnO/TiO_2 decreased with increasing of contents of zinc. The added ZnO role was based on the crystal growth inhibiter, which leading to small grain size related with increasing of surface area. In addition, inductively coupled plasma atomic emission spectroscopy (ICP-AES) was used to consider the amount of Zn on Ti catalyst. The results of ICP analysis found that the contents of Zn more than the nominal value may because the preparation of mixed oxide sol.

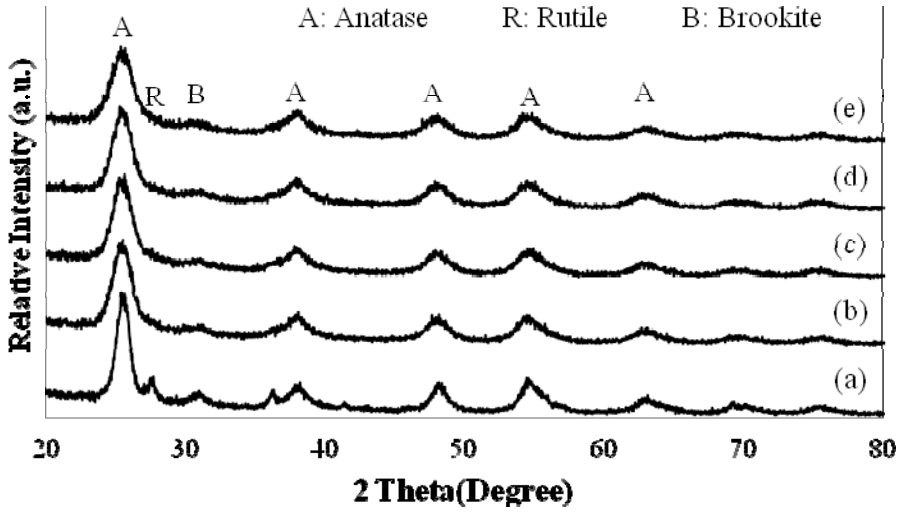

Figure 5.5 XRD patterns of ZnO/TiO_2 powders at various percentages of ZnO (a) 0 wt %, (b) 1.0 wt %, (c) 3.0 wt % (d) 5.0 wt % and (e) 7.0 wt %

Table 5.7 Crystalline size, surface area and weight fraction of anatase, rutile and brookite of ZnO/TiO_2 powders calcined at 400°C for 2 hours

Zn/Ti (wt%)	Crystallite size (nm)	Surface area (m^2/g)	Amount of Zr from ICP (wt%)	W_A	W_R	W_B
Pure TiO_2	6.1	77	-	0.51	0.19	0.30
1.0	4.1	120	1.81	0.52	0.17	0.31
3.0	3.9	117	3.42	0.50	0.17	0.33
5.0	3.7	122	5.70	0.50	0.16	0.34
7.0	3.0	130	7.38	0.46	0.18	0.36

Table 5.8 reported energy band gap of TiO_2 and TiO_2 modified by ZnO. The results indicated that the addition of ZnO enhanced energy band gap when compare with pure TiO_2. The energy band gap of ZnO/TiO_2 enhanced with increasing of content of ZnO and decreased when content of ZnO up to 5% wt. The ZnO/TiO_2 5% wt had the widest energy band gap so it affected to increase the light adsorption of dye.

Moreover, the amount of dye adsorbed on the TiO_2 and ZnO/TiO_2 electrodes were presented in Figure 5.6. The amount of dye adsorbed on ZnO/TiO_2 electrodes increased when contents of ZnO increased, compared with pure TiO_2 electrode.

Table 5.8 The comparison band gap from UV-vis spectra of titanium dioxide doped with various amount of Zincoxide calcined at 400°C for 2 hours.

Sample	Wavelength (nm)	Band gap energy (eV)
Pure TiO_2	415	3.00
ZnO_2/TiO_2 1.0%wt	410	3.03
ZnO_2/TiO_2 3.0%wt	406	3.06
ZnO_2/TiO_2 5.0%wt	400	3.11
ZnO_2/TiO_2 7.0%wt	402	3.09

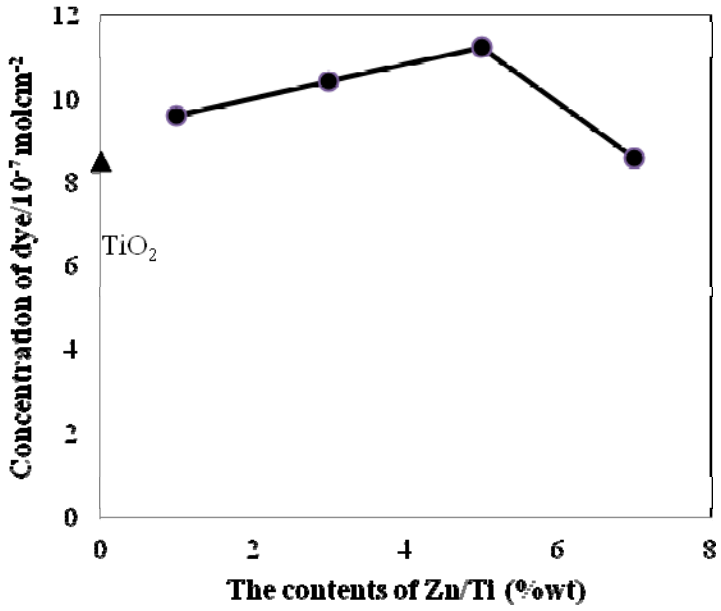

Figure 5.6 Relationship between concentrations of dye with various contents of ZnO/TiO_2

The TiO_2 and ZnO/TiO_2 electrodes layer were prepared by ultrasonic spray coating on FTO substrate. The electrode layer was sintered at 400^{o}C for two hours. The amount of ZnO was varied from 0 to 7% (w/w). The photovoltaic properties were measured by the I-V tester under AM 1.5 irradiation. The observed I-V characteristics

was tabulated in the Table 5.9 the corresponding solar cell parameters**.** Modification of TiO_2 electrode with ZnO gave rise to higher cell efficiency. The highest cell efficiency of 6.55±0.10% was obtained with a DSSC with 5wt% ZnO/TiO_2 electrode. The current density enhanced from 7.90±0.80 to 9.52±0.29 $mA \cdot cm^{-2}$ for 5wt% of ZnO/TiO_2 electrode compare with pure TiO_2 electrode. This was in agreement the amount of dye adsorbed on the surface of the electrode (see in Figure 5.5). When the content of ZrO_2 was enhanced to 7.0 wt %, the amount of the dye adsorbed shows decrease with the increase of ZnO content, which will result in the decrease of the light harvesting efficiency.

Table 5.9 Electrochemical properties of dye-sensitized solar cell of ZnO/TiO_2 electrode calcined at 400°C for 2 hours with 500 coats

ZnO/TiO_2 (wt%)	V_{OC} (Volt)	J_{SC} ($mA \cdot cm^{-2}$)	Fill Factor	Efficiency (%)
TiO_2	0.74±0.01	7.90±0.80	0.81±0.06	4.77±0.48
1.0	0.75±0.01	7.51±0.28	1.00±0.04	5.62±0.09
3.0	0.75±0.01	8.40±0.20	0.98±0.03	6.22±0.07
5.0	0.75±0.01	9.52±0.29	0.92±0.03	6.55±0.10
7.0	0.76±0.02	6.48±0.19	0.96±0.05	4.71±0.09

5.2 Dye-sensitized solar cell using double-layered conduction glass

The electrode layer was deposited onto conducting glass by the layer-by-layer deposition of double-layered TiO_2 particles. The layer was spray-coated on FTO glass substrates 500 times using an ultrasonic spray coater. Next, the electrodes were sintered at 400°C for two hours. It is expected that the double layer film electrode can be extended to other composite films with different layer structures and morphologies for enhancing the efficiencies of DSSC.

Type A: Deposition ZrO_2/TiO_2 7.0 wt % sol on a FTO glass substrate, the numbers of coats were 500 times and calcined at 400°C for two hours. The content of Zr gave the highest efficiency for dye sensitized solar cell.

Type B: Deposition pure TiO_2 sols on a FTO glass substrate, the number of coats were 250 times and then calcined at 400°C for two hours. Next, the deposition process of the mixed oxide electrode ZrO_2/TiO_2 7.0 wt % was to obtain the desired film thickness same single-layer electrode. The electrode was finally calcined at 400°C for 30 minutes.

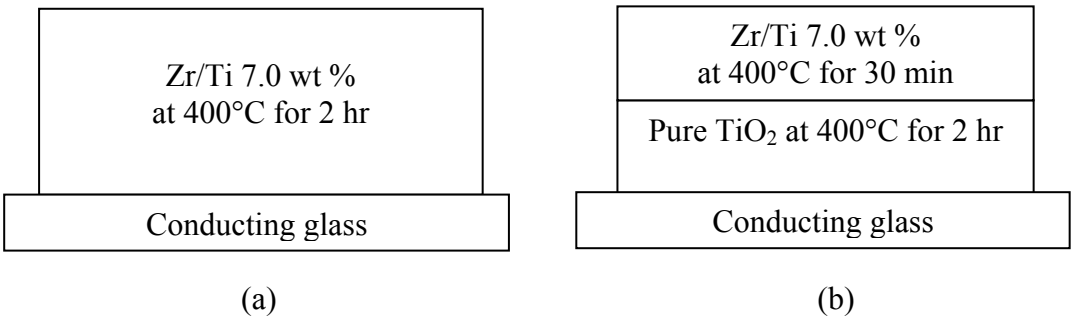

Figure 5.12 Type of the mixed oxide electrode on conducting glass prepared for DSSC (a) Single-layer structure and (b) Double-layers structure

Then the electrodes were immersed in 0.5 mM of the ruthenium complex dye solution, cis-bis(isothiocyanato)bis(2,2'-bipyridyl- 4, 4' -dicarboxylato)-ruthenium (II) or N3 dye, at room temperature for 24 hours. Then the electrodes were sequentially dried with hair dryer. The UV-visible spectrophotometer was used for measure the amount of the dye concentration which the dye was desorbed from TiO_2 electrode into NaOH solution in ethanol. Table 5.10 showed the concentration of dye adsorption on electrodes of single layer and double layer electrode structure. The adsorption of dye in single layered and double layered are 15.73×10^{-7} mol·cm^{-2} and 12.68×10^{-7} mol·cm^{-2}, respectively

Table 5.10 The properties of electrodes calcined at various temperatures

	Calcined temperature (°C)	Crystallite size (nm)	Surface area (m^2/g)	Concentration of dye ($mol \cdot cm^{-2}$)
Single-layer : ZrO_2/TiO_2 7.0 wt %	400°C 120 min	4.6	115	15.73×10^{-7}
Double-layers : Pure TiO_2 (underlayer)	400°C 120 min	6.3	77	
ZrO_2/TiO_2 7.0 wt % (overlayer)	400°C 30 min	3.4	126	12.68×10^{-7}

Figure 5.13 shows the diffused reflection spectra of single-layer and double-layer electrode. The diffused reflectance of the films enhances as the light scatting layer were added which effect to increasing of performance of cell.

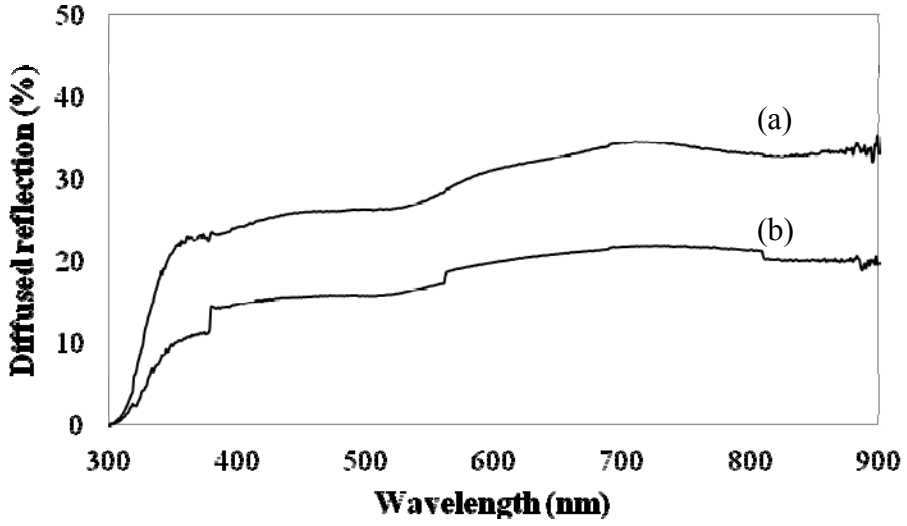

Figure 5.13 Diffused reflection of electrode layer
(a) Single-layer and (b) Double-layer

Table 5.11 compared the properties and photovoltaic parameters of single layered and double layered thin film electrode. The photovoltaic properties were measured by the I-V tester under AM 1.5 irradiation and using a xenon lamp under an intensity of 100 mW/cm^2. The DSSC was improved performance by using double-layered electrode structure because it had light scattering. The use of the light scattering layers resulted in an increase the J_{sc} value from 8.48±0.57 to 13.58±0.63 mA·cm^{-2} and the overall energy conversion efficiency was enhanced from 6.57±0.26% to 9.28±0.34% (Lee al et., 2009).

Table 5.11 DSSC performance of single and double layers electrode

	V_{oc} (volt)	J_{sc} (mA·cm^{-2})	Fill Factor	Efficiency (%)
Single-layer : ZrO_2/TiO_2 7.0 wt %	0.74±0.00	8.48±0.57	1.05±0.06	6.57±0.26
Double-layers : Pure TiO_2 (under) ZrO_2/TiO_2 7.0 wt % (over)	0.74±0.004	13.58±0.63	0.92±0.02	9.28±0.34

CHAPTER VI

CONCLUSIONS AND RECOMMENDATIONS FOR FUTURE RESEARCH

This research focuses mainly on the improvement the power conversion efficiency of DSSC by modifying TiO_2 electrode. Another oxide, ZrO_2, CeO_2, or ZnO was mixed with TiO_2 sol for preparing thin film electrode. The double layer structure was investigated including the effects of several preparation parameters on the cell efficiency. In this chapter, section 6.1 provided the conclusion that obtained from the experimental results of the effect of the modification of TiO_2 electrode layer by adding ZrO_2, CeO_2 and ZnO includes double-layer TiO_2 films on the performance of dye-sensitized solar cell. Additionally, in section 6.2 provided the recommendations for future study.

6.1 Conclusions

6.1.1 Modification of TiO_2 electrode layer by adding ZrO_2

The modification of TiO_2 electrode by ZrO_2 role was based on the crystal growth inhibited leading to increase surface area when compared with pure TiO_2, which affect to the higher the amount of dye adsorbed in ZrO_2/TiO_2 electrode. Resulting dye molecules adhesive on the surface more. Lead to improved short circuit current density (J_{SC}) and the efficiency of the cells when compared to cells with only TiO_2. The addition of ZrO_2 improved the overall cell efficiency from 4.77±0.48% for pure TiO_2 electrode to 6.57±0.26% for 7 wt% ZrO_2/TiO_2 electrode calcined at 400 ^oC for two hours.

6.1.2 Modification of TiO_2 electrode layer by adding CeO_2

The addition of CeO_2 lowered the cell efficiency, which was probably due to lower amount of dye adsorption. The amount of dye adsorption decreased, resulting in reduced short circuit current density (J_{SC}) and efficiency of the cell decreased when compared to cells with pure TiO_2.

6.1.3 Modification of TiO_2 electrode layer by adding ZnO

The modification of TiO_2 electrode by ZnO increased surface area when compared with pure TiO_2, which affect to the higher the amount of dye adsorbed in ZnO/TiO_2 electrode. Resulting dye molecules adhesive on the surface more. Lead to improved short circuit current density (J_{SC}) and the efficiency of the cells when compared to cells with only TiO_2. The highest cell efficiency of 6.55±0.10% was obtained for the DSSC with 5wt% ZnO/TiO_2 electrode calcined at 400 ^{o}C for two hours.

6.1.4 Double-layered TiO_2 electrode

Double layer structure was improved the light scattering and the overall energy conversion efficiency was enhanced from 6.57±0.26% to 9.28±0.34% when compare with single-layered ZrO_2/TiO_2 electrode.

6.2 Recommendations for future studies

From the previous conclusions, the following recommendations for future studies are proposed.

1. Improving the amount of dye adsorption on TiO_2 electrode for increasing the overall efficiency of DSSC.
2. Improving the surface area of TiO_2 electrode with other metal oxide.
3. Enhance the light harvest efficiency of dye-adsorbed TiO_2 electrodes by improving the structure of electrode was multi-layer electrode

REFERENCES

Amornpitoksuk, P. and Leesakul, N., Dye Sensitized Solar Cell, DSSC. Songklanakarin J. Sci. Technol. 25(4) (2003): 535-551.

Bak, Y.R., Kim, G.O., Hwang, M.J., Cho, K.K., Kim, K.W., and Ryu, K.S., Fabrication and performance of nanoporous TiO_2/SnO_2 electrodes with a half hollow sphere structure for dye densitized solar cells. Springer: J Sol-Gel Sci Technol (2011).

Chang, H., Su, H.T., Chen, W.A., Huang, K.D., Chien, S.H., Chen, S.L., and Chen, C.C., Fabrication of multilayer TiO_2 thin films for dye-sensitized solar cells with high conversion efficiency by electrophoresis deposition. Solar Energy 84 (2010): 130–136.

Chen, G., Zheng, K., Mo, X., Sun, D., Meng, Q., and Chen, G. Metal-free indoline dye sensitized zinc oxide nanowires solar cell. Journal of Materials Letters 64 (2010): 1336-1339.

Chen, L., Tan, W., Zhang, J., Zhou, X., Zhang, X., and Lin, Y., Fabrication of high performance Pt counter electrodes on conductive plastic substrate for flexible dye-sensitized solar cells. Electrochimica Acta 55 (2010): 3721–3726.

Chen, Y.S., Lee, J.N., Tsai, S.Y., and Ting, C.C., Manufacture of Dye-Sensitized Nano Solar Cells and their I-V Curve Measurements. Proceedings of ICAM (2007).

Chiba, Y., Islam, A., Watanabe, Y., Komiya, R., Koide, N.and Han, L., Dye-Sensitized Solar Cells with Conversion Efficiency of 11.1%. Japanese Journal of Applied Physics 45 (2006): L638–L640.

Chou, C.S., Chou, F.C., and Ka, J.Y., Preparation of ZnO-coated TiO_2 electrodes using dip coating and their applications in dye-sensitized solar cells. Powder Technology 215-216 (2012): 38–45.

Grätzel, M., Review: Dye-sensitized solar cells. Journal of Photochemistry and Photobiology C: Photochemistry Reviews4 (2003): 145–153.

Hagfeldt, A., Working electrodes and counter electrodes. Uppsala Universitet (2011).

Han, C.H., Lee, H.S., Lee, K.W., Han, S.D., and Singh, I., Synthesis of Amorphous Er^{3+}-Yb^{3+} Co-doped TiO_2 and Its Application as a Scattering Layer for Dye-sensitized Solar Cells, Bull. Korean Chem. Soc. 30 (2009): 219-223.

Harizanova, O., and Harizanova, A., Development and investigation of sol-gel solutions for the formation of TiO_2 coatings. Solar Energy Materials & Solar Cells 63 (2000): 185-195.

Kao, M.C., Chen, H.Z., and Young, S.L., Effects of ZnO coating on the performance of TiO_2 nanostructured thin films for dye-sensitized solar cells. Applied Physics A: Materials Science & Processing (2009): 469-474.

Karthikeyan, C.S., Thelakkat, M., and Willert-Porad, M., Different mesoporous titania films for solid-state dye sensitised solar cells. Thin Solid Films 511 – 512 (2006): 187 – 194.

Kim, J.Y., Lee, S., Noh, J.H., Jung, H.S., and Hong, K.S., Enhanced photovoltaic properties of overlayer-coated nanocrystalline TiO_2 dye-sensitized solar cells (DSSCs). J Electroceram 23 (2009): 422–425.

Kim, S.S., Yum, J.H., and Sung, Y.E., Flexible dye-sensitized solar cells using ZnO coated TiO_2 nanoparticles. Journal of Photochemistry and Photobiology A: Chemistry 171 (2005): 269–273.

Kitiyanan, A., Ngamsinlapasathian, S., Pavasupree, S., and Yoshikawa, S., The preparation and characterization of nanostructureed TiO_2-ZrO_2 mixed oxide electrode for efficient dye-sensitized solar cells. Journal of Solids State Chemistry 178 (2005): 1044-1048.

Kitiyanan, A., Sukulkhaemaruethai, S., Suzuki, Y., and Yoshikawa, S., Structural and photovoltaic properties of binary TiO_2-ZrO_2 oxides system prepared by sol-gel method. Composites Science and Technology 66 (2006): 1259-1265.

Kong, F.T., Dai, S.Y., and Wang, K.J., Review Article: Review of Recent Progress in Dye-Sensitized Solar Cells. Hindawi Publishing Corporation: Advances in OptoElectronics (2007).

Lee, C.P., Chen, P.Y., and Ho, K.C., Ionic Liquid Based Electrolytes for Dye-Sensitized Solar Cells. Ionic Liquids: Theory, Properties, New Approaches (2011): 631-656.

Lee, J.K., Jeong, B.H., Jang, S.I., Yeo, Y.S., Park, S.H., Kim, J.U., Kim, Y.G., Jang, Y.W., and Kim, M.R., Multi-layered TiO_2 nanostructured films for dye-sensitized solar cells. J Mater Sci: Mater Electron20 (2009): S446–S450.

Lenzmann, F. O., and Kroon, J.M., Review Article: Recent Advances in Dye-Sensitized Solar Cells. Hindawi Publishing Corporation Advances in OptoElectronics (2007).

Menzies, D., Cervini R., Cheng, Y.B., and Simon, G.P., Nanostructured ZrO_2-Coared TiO_2 Electrodes for Dye-Sensitized Solar Cells. Journal of Sol-Gel Science and Technology 32 (2004): 363-366.

Menzies, D., Dai, Q., Cheng, Y.B., Simon, G.P., and Spiccia, L., Improvement of the Zirconia sell in nanostructureed titania core-shell working electrodes for dye-sensitized solar cells. Material Letter 59 (2005): 1893-1896.

O'regan, B. and Grätzel, M., A low-cost, high-efficiency solar cell based on dye-sensitized colloidal TiO_2 films. Nature Publishing Group: Letters to nature 353 (1991): 737-740.

Porkodi, K. and Arokiamary, S., Synthesis and spectroscopic characterization of nanostructured anatase titania. Materials Characterization 58 (2007): 495–503.

Rochford, J., Chu, D., Hagfeldt, A., and Galoppin, E., Tetrachelate Porphyrin Chromophores for Metal Oxide Semiconductor Sensitization: Effect of the Spacer Length and Anchoring Group Position. J. AM. CHEM. SOC. 129 (2007): 4655-4665.

Shanmugam, M., Bills, B., Baroughi, M.F., and Galipeau, D., ELECTRON TRANSPORT IN DYE SENSITIZED SOLAR CELLS WITH TiO_2/ZnO CORESHELL PHOTOELECTRODE. IEEE (2010): 3256-3259.

Wang, M., Huang, C., Cao, Y., Yu, Q., Deng, Z., Liu, Y., Huang, Z., Huang, J., Huang, Q., Guo, W., and Liang, J., Dye-sensitized solar cells based on nanoparticle-decorated ZnO/TiO_2 core/shell nanorod arrays. J. Phys. D: Appl. Phys. 42 (2009).

Wang, Z.S., Kawauhi, H., Kashima, T., and Arakawa, H., Significant influence of TiO_2 photoelectrode morphology on the energy conversion efficiency of N719 dye-sensitized solar cell. Coordination Chemistry Reviews 248 (2004): 1381-1389.

Xu, H., Tao, X., Wang, D.T., Zheng, Y.Z., and Chen, J.F., Enhanced efficiency in dye-sensitized solar cells based on TiO_2 nanocrystal/nanotube double-layered films. Electrochimica Acta 55 (2010): 2280–2285.

Yong, L., Hui, S., and Youjun, D., Study on the improved structure of dye-sensitized solar cells for enhancing light absorption. Front. Mater. Sci. China 1(3) (2007): 293–296

APPENDICES

APPENDIX A

CALCULATION OF THE CRYSTALLITE SIZE

Calculation of the crystalline size by Debye-Scherrer equation

The crystalline size can be calculated from the width at half-height of the diffraction peak of XRD pattern using the Debye-Scherrer equation

From Scherrer equation

$$D = \frac{k\lambda}{\beta\cos\theta} \qquad \text{(A. 1)}$$

where D = Crystallite size, Å

K = Crystalline-shape factor = 0.9

λ = X-ray wavelength, 1.5418 Å for CuKα

θ = Observed peak angle, degree

β = X-ray diffraction broadening, radian

The X-ray diffraction broadening (β) is the pure width of the powder diffraction, free of all broadening due to the experimental equipment. Standard α-alumina is used to observe the instrumental broadening since its crystallite size is larger than 2000Å. The X-ray diffraction broadening (β) can be obtained by using Warren's formula.

From Warren's formula:

$$\beta^2 = B_M^2 - B_S^2 \qquad \text{(A. 2)}$$

$$\beta = \sqrt{B_M^2 - B_S^2}$$

Where B_M = Measured peak width in radians at half peak height

B_S = Corresponding width of a standard material

Example: calculation of the crystallite size of TiO_2

The half-height width of (101) diffraction peak = 1.0659°

= 0.018594 radian

The corresponding half-height width of peak of TiO_2 = 0.003836 radian

The pure width = $\sqrt{B_M^2 - B_S^2}$

= $\sqrt{0.018584^2 - 0.003836^2}$

= 0.0182 radian

β = 0.0182 radian

2θ = 25.55°

θ = 12.775°

λ = 1.5418 Å

$$\text{The crystallite size} = \frac{0.9\times1.5418}{0.0182\cos12.775} = 78.18\ \text{Å} = 7.82\ \text{nm}$$

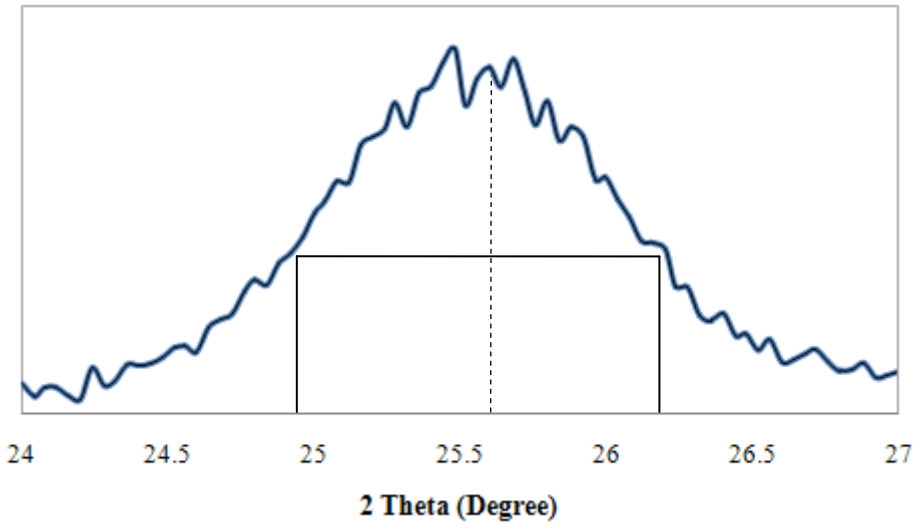

Figure A.1 The (101) diffraction peak of TiO_2 for calculation of the crystallite size

APPENDIX B

CALCULATION OF WEIGHT FRACTION OF ANATASE, RETILE AND BROOKITE PHASE

The phase content of a sable were determined by XRD which can be calculated from the integrated intensities at 2θ values of 25.32°, 27.44°, and 30.88° corresponded to the anatase, rutile and brookite phase, respectively.

The weight fraction of the phase content can be calculated by (Zhang, Banfield, 2000) as follows:

$$W_A = \frac{k_A A_A}{k_A A_R + A_R + k_B A_B}$$

#

$$W_R = \frac{A_R}{k_A A_R + A_R + k_R A_R}$$

#

$$W_B = \frac{k_B A_B}{k_A A_R + A_R + k_B A_B}$$

Where

W_A = weight fraction of anatase

W_R = weight fraction of rutile

W_B = weight fraction of brookite

A_A = the intensity of the anatase peak

A_R = the intensity of the rutile peak

A_B = the intensity of the brookite peak

k_A = the coefficients factor of anatase was 0.886

k_B = the coefficients factor of rutile was 2.721

Example: calculation of the phase contents of ZrO_2/TiO_2 calcined 400°C for two hours

Where

The integrated intensities of anatase (A_A) = 375

The integrated intensities of rutile (A_R) = 64

The integrated intensities of brookite (A_B) = 53

The weight fraction of the phase content can be calculated by (Zhang, Banfield, 2000) as follows:

$$W_A = \frac{0.886(375)}{0.886(375) + (64) + 2.721(53)} = 0.61$$

$$W_R = \frac{64}{0.886(375) + (64) + 2.721(53)} = 0.12$$

$$W_B = \frac{2.721(53)}{0.886(375) + (64) + 2.721(53)} = 0.27$$

APPENDIX C

DETERMINATION OF THE AMOUNT OF DYE ADSORBED ON TITANIA SURFACE

The amount of dye adsorbed was determined by UV-Visible Absorption Spectroscopy (UV-Vis) where measuring the concentration of dye desorbed on the titania film into a mixed solution of 0.1M NaOH and ethanol at a volume ratio 1:1.

The calibration curve of the concentration of dye with absorbance was illustrated in the following figure.

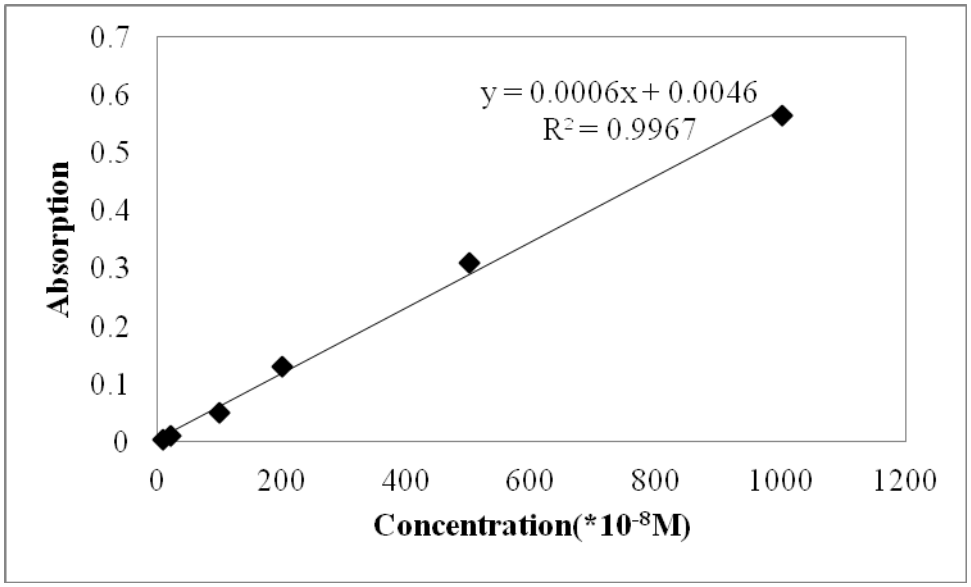

Figure C.1 The calibration curve of the concentration of N3 dye adsorbed

APPENDIX D

THE CALCULATION OF THE BAND GAP FROM UV-VIS SPECTRA

The band gap (E_g) of the sample was determined by the following equation (Eq.C1):

$$E_g = \frac{hC}{\lambda} \qquad \text{(Eq.C1)}$$

Where E_g is the band gap (eV)

h = Planks constant = 6.626×10^{-34} Joules sec

C= Speed of light = 3.0×10^{8} meter/sec

λ = Cut off wavelength (meters)

1 eV = 1.6×10^{-19} Joules (conversion factor)

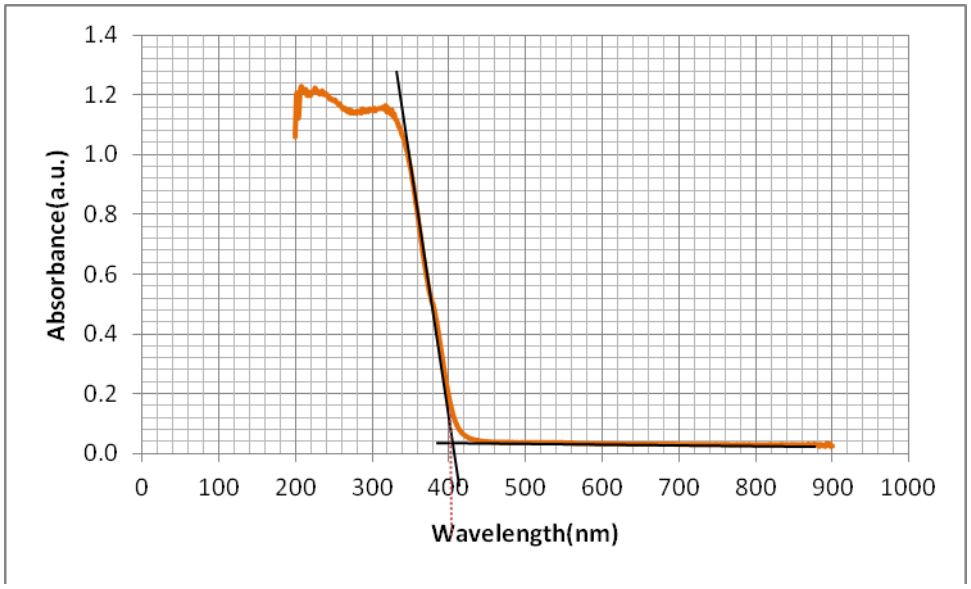

Figure C.2 UV-visible absorption characteristics of titanium dioxide

The spectral data recorded showed the strong cut off at 415 nm; where the absorbance value is a minimum.

Calculation

$$E_g = \frac{hC}{\lambda}$$

$$E_g = \frac{(6.63\times10^{-34}\,Joules\cdot\sec)(3.0\times10^{8}\,meter/\sec)}{(415\times10^{-9}\,meters)(1.6\times10^{-19}\,Joules)} = 3.0 \text{ eV}$$

APPENDIX E

CALCULATION OF RESULT OF ICP-OES

Calculation of ICP-OES results

The results from ICP-OES characterization were calculation the contents of metal in catalysts. The example of calculation is as following:

Example: calculation of the contents of 1.0 wt % of Zr/Ti in ZrO_2/TiO_2 powder.

For 1.0 wt % of Zr/Ti powder, the initial weight of powder was 0.0105 g.

Hence, the calculation of the zirconium contents the catalysts as follows:

The amounts of zirconium in the catalyst were;

In 100 g of the ZrO_2/TiO_2, had a zirconium content was 1.0 %

In 0.0105 g of the ZrO_2/TiO_2, had a zirconium content was $\frac{0.0105 \times 1.0}{100}$

$= 0.00105$ mg

For digest a samples were diluted to 10 cm^3 of volume

Therefore;

The sample had a concentration were $= \frac{0.0105 \times 1000}{10} = 1.05$ ppm

From the result of ICP-OES, shown the contents of zirconium was 1.008 ppm

Therefore;

The zirconium contents in the catalysts were calculated by

The zirconium concentrations were 1.05 ppm refer 1.0 wt % of zirconium in catalyst.

The zirconium concentrations were 1.008 ppm refer $\frac{1.008 \times 1.0}{1.05}$

= 0.96 wt % of zirconium in the catalyst

APPENDIX F

THE ELECTROCHEMICAL PROPERTIES OF DYE-SENSITIZED SOLAR CELL

The electrochemical properties of dye-sensitized solar cell as a thickness and sintering temperature of TiO_2, ZrO_2/TiO_2, CeO_2/TiO_2, and ZnO/TiO_2 electrode by I-V tester. In this study three samples were used, and the efficiency of cell given is the average value follow by the standard derivation.

Table E.1 Electrochemical properties of dye-sensitized solar cell of TiO_2 electrode calcined at 400°C for 2 hours with 500 coats

Number of cell	V_{OC} (Volt)	J_{SC} ($mA \cdot cm^{-2}$)	Fill Factor	Efficiency (%)
1	0.75	7.04	0.86	4.54
2	0.75	8.18	0.88	5.46
3	0.75	7.29	0.76	4.16
4	0.72	9.08	0.75	4.94
Average	0.74±0.01	7.90±0.80	0.81±0.06	4.78±0.48

Table E.2 Electrochemical properties of dye-sensitized solar cell of 1.0%wt of ZrO_2/TiO_2 electrode calcined at 400°C for 2 hours with 500 coats

Number of cell	V_{OC} (Volt)	J_{SC} ($mA \cdot cm^{-2}$)	Fill Factor	Efficiency (%)
1	0.65	8.32	1.04	5.65
2	0.73	8.01	0.91	5.31
3	0.74	5.72	1.01	4.28
Average	0.71±0.04	7.35±1.16	0.99±0.06	5.08±0.58

Table E.3 Electrochemical properties of dye-sensitized solar cell of 3.0%wt of ZrO_2/TiO_2 electrode calcined at 400°C for 2 hours with 500 coats

Number of cell	V_{OC} (Volt)	J_{SC} ($mA \cdot cm^{-2}$)	Fill Factor	Efficiency (%)
1	0.66	9.10	0.89	5.31
2	0.74	10.05	0.78	5.78
3	0.71	9.39	0.91	6.05
Average	0.70±0.03	9.51±0.40	0.86±0.06	5.71±0.31

Table E.4 Electrochemical properties of dye-sensitized solar cell of 5.0%wt of ZrO_2/TiO_2 electrode calcined at 400°C for 2 hours with 500 coats

Number of cell	V_{OC} (Volt)	J_{SC} ($mA \cdot cm^{-2}$)	Fill Factor	Efficiency (%)
1	0.73	7.39	1.03	5.57
2	0.72	8.18	1.00	5.88
3	0.75	6.00	1.21	5.43
Average	0.74±0.01	7.19±0.90	1.08±0.09	5.63±0.19

Table E.5 Electrochemical properties of dye-sensitized solar cell of 7.0%wt of ZrO_2/TiO_2 electrode calcined at 400°C for 2 hours with 500 coats

Number of cell	V_{OC} (Volt)	J_{SC} ($mA \cdot cm^{-2}$)	Fill Factor	Efficiency (%)
1	0.74	9.27	1.00	6.85
2	0.74	7.98	1.06	6.24
3	0.74	8.17	1.09	6.63
Average	0.74±0.00	8.48±0.57	1.05±0.06	6.57±0.26

Table E.6 Electrochemical properties of dye-sensitized solar cell of 10.0%wt of ZrO_2/TiO_2 electrode calcined at 400°C for 2 hours with 500 coats

Number of cell	V_{OC} (Volt)	J_{SC} ($mA \cdot cm^{-2}$)	Fill Factor	Efficiency (%)
1	0.74	7.42	1.00	5.51
2	0.74	5.84	0.87	3.76
3	0.77	4.84	1.09	4.07
Average	0.75±0.01	6.03±1.06	0.99±0.09	4.45±0.76

Table E.7 Electrochemical properties of dye-sensitized solar cell of 1.0%wt of CeO_2/TiO_2 electrode calcined at 400°C for 2 hours with 500 coats

Number of cell	V_{OC} (Volt)	J_{SC} ($mA \cdot cm^{-2}$)	Fill Factor	Efficiency (%)
1	0.69	6.34	0.82	3.57
2	0.71	6.02	0.94	3.98
3	0.70	6.16	0.94	4.06
Average	0.70±0.01	6.17±0.13	0.90±0.06	3.87±0.21

Table E.8 Electrochemical properties of dye-sensitized solar cell of 3.0%wt of CeO_2/TiO_2 electrode calcined at 400°C for 2 hours with 500 coats

Number of cell	V_{OC} (Volt)	J_{SC} ($mA \cdot cm^{-2}$)	Fill Factor	Efficiency (%)
1	0.56	0.48	0.41	0.11
2	0.62	0.51	0.56	0.18
3	0.62	0.57	0.52	0.18
Average	0.60±0.03	0.52±0.04	0.50±0.06	0.16±0.03

Table E.9 Electrochemical properties of dye-sensitized solar cell of 5.0%wt of CeO_2/TiO_2 electrode calcined at 400°C for 2 hours with 500 coats

Number of cell	V_{OC} (Volt)	J_{SC} ($mA \cdot cm^{-2}$)	Fill Factor	Efficiency (%)
1	0.53	0.45	0.45	0.11
2	0.52	0.43	0.38	0.09
3	0.51	0.42	0.45	0.10
Average	0.52±0.01	0.44±0.01	0.43±0.03	0.10±0.01

Table E.10 Electrochemical properties of dye-sensitized solar cell of 7.0%wt of CeO_2/TiO_2 electrode calcined at 400°C for 2 hours with 500 coats

Number of cell	V_{OC} (Volt)	J_{SC} ($mA \cdot cm^{-2}$)	Fill Factor	Efficiency (%)
1	0.48	0.50	0.36	0.09
2	0.48	0.37	0.37	0.07
3	0.49	0.41	0.33	0.07
Average	0.49±0.01	0.43±0.06	0.35±0.02	0.07±0.01

Table E.11 Electrochemical properties of dye-sensitized solar cell of 1.0%wt of ZnO/TiO_2 electrode calcined at 400°C for 2 hours with 500 coats

Number of cell	V_{OC} (Volt)	J_{SC} ($mA \cdot cm^{-2}$)	Fill Factor	Efficiency (%)
1	0.74	7.23	1.02	5.50
2	0.76	7.89	0.95	5.69
3	0.75	7.40	1.03	5.67
Average	0.75±0.01	7.51±0.28	1.00±0.04	5.62±0.09

Table E.12 Electrochemical properties of dye-sensitized solar cell of 3.0%wt of ZnO/TiO_2 electrode calcined at 400°C for 2 hours with 500 coats

Number of cell	V_{OC} (Volt)	J_{SC} ($mA \cdot cm^{-2}$)	Fill Factor	Efficiency (%)
1	0.76	8.55	0.94	6.13
2	0.74	8.54	0.99	6.28
3	0.75	8.11	1.02	6.24
Average	0.75±0.01	8.40±0.20	0.98±0.03	6.22±0.07

Table E.13 Electrochemical properties of dye-sensitized solar cell of 5.0%wt of ZnO/TiO_2 electrode calcined at 400°C for 2 hours with 500 coats

Number of cell	V_{OC} (Volt)	J_{SC} ($mA \cdot cm^{-2}$)	Fill Factor	Efficiency (%)
1	0.74	9.48	0.95	6.69
2	0.75	9.89	0.87	6.48
3	0.76	9.19	0.93	6.47
Average	0.75±0.01	9.52±0.29	0.92±0.03	6.55±0.10

Table E.14 Electrochemical properties of dye-sensitized solar cell of 7.0%wt of ZnO/TiO_2 electrode calcined at 400°C for 2 hours with 500 coats

Number of cell	V_{OC} (Volt)	J_{SC} ($mA \cdot cm^{-2}$)	Fill Factor	Efficiency (%)
1	0.78	6.75	0.90	4.74
2	0.73	6.38	0.98	4.59
3	0.75	6.42	1.01	4.80
Average	0.76±0.02	6.48±0.19	0.96±0.05	4.71±0.09

Table E.15 Electrochemical properties of dye-sensitized solar cell of double-layers electrode of ZrO_2/TiO_2 film

Number of cell	V_{OC} (Volt)	J_{SC} ($mA \cdot cm^{-2}$)	Fill Factor	Efficiency (%)
1	0.74	12.77	0.96	9.13
2	0.73	14.09	0.90	9.34
3	0.74	13.18	0.90	8.85
4	0.74	14.29	0.93	9.78
Average	0.74±0.004	13.58±0.63	0.92±0.02	9.28±0.34

VITA

Miss Anchana Kittitanesuan was born on December 20, 1987 in Chonburi, Thailand. She finished high school from Sriracha School, Chonburi, and received the bachelor's degree of Chemical Engineering, Burapha University, Chonburi. The she continued her master degree in Chemical Engineering at Chulalongkorn University.

Anchana Kittitanesuan and Akawat Sirisuk. Dye-sensitizer solar cells with TiO_2 electrode modified by ZrO_2, or CeO_2. Proceeding of pure and applied chemisty international conference, Chiang Mai University, Chiang Mai, Thailand. Jan. 11-13, 2012 (PACCON2012).